Coupling and cooperativity in voltage activation of a limited-state BK channel gating in saturating Ca^{2+}

Christopher Shelley,[1,2] Xiaowei Niu,[1] Yanyan Geng,[1] and Karl L. Magleby[1,2]

[1]Department of Physiology and Biophysics and [2]Neuroscience Program, University of Miami Miller School of Medicine, Miami, FL 33136

Voltage-dependent gating mechanisms of large conductance Ca^{2+} and voltage-activated (BK) channels were investigated using two-dimensional maximum likelihood analysis of single-channel open and closed intervals. To obtain sufficient data at negative as well as positive voltages, single-channel currents were recorded at saturating Ca^{2+} from BK channels mutated to remove the RCK1 Ca^{2+} and Mg^{2+} sensors. The saturating Ca^{2+} acting on the Ca^{2+} bowl sensors of the resulting BK_B channels increased channel activity while driving the gating into a reduced number of states, simplifying the model. Five highly constrained idealized gating mechanisms based on extensions of the Monod-Wyman-Changeux model for allosteric proteins were examined. A 10-state model without coupling between the voltage sensors and the opening/closing transitions partially described the voltage dependence of Po but not the single-channel kinetics. With allowed coupling, the model gave improved descriptions of Po and approximated the single-channel kinetics; each activated voltage sensor increased the opening rate approximately an additional 23-fold while having little effect on the closing rate. Allowing cooperativity among voltage sensors further improved the description of the data: each activated voltage sensor increased the activation rate of the remaining voltage sensors approximately fourfold, with little effect on the deactivation rate. The coupling factor was decreased in models with cooperativity from ~23 to ~18. Whether the apparent cooperativity among voltage sensors arises from imposing highly idealized models or from actual cooperativity will require additional studies to resolve. For both cooperative and noncooperative models, allowing transitions to five additional brief (flicker) closed states further improved the description of the data. These observations show that the voltage-dependent single-channel kinetics of BK_B channels can be approximated by highly idealized allosteric models in which voltage sensor movement increases Po mainly through an increase in channel opening rates, with limited effects on closing rates.

INTRODUCTION

Large conductance Ca^{2+}-activated K^+ (BK) channels are activated by membrane depolarization and intracellular Ca^{2+} and Mg^{2+} (Latorre and Brauchi, 2006; Lu et al., 2006; Salkoff et al., 2006; Cui et al., 2009; for review see Magleby, 2003). Once activated, the K^+ efflux through the opened channel drives the membrane potential in the negative direction. Through this mechanism, BK channels sense both depolarization and intracellular divalent cations to control membrane excitability through a negative feedback loop. BK channels are tetramers comprised of four pore-forming α subunits (Adelman et al., 1992). The membrane-spanning segments S1–S6 of the α subunits share similarities with the family of voltage-gated K^+ channels (Butler et al., 1993). In addition to S1–S6, the BK channel α subunit has a unique S0 transmembrane segment (Meera et al., 1997) as well as a large cytoplasmic C terminus thought to form a Ca^{2+}-activated gating ring comprised of eight RCK (regulators of the conductance of potassium) domains, two per subunit, designated as RCK1 and RCK2 (Jiang et al., 2001, 2002). Each RCK1 domain, which is connected to the S6 gates through a nonconserved linker, has a high affinity Ca^{2+} binding site, the RCK1 site defined by D362/D367, and a low affinity (millimolar) Mg^{2+} site defined by E399/E374 (Xia et al., 2002; Shi et al., 2002; Yang et al., 2008). Each RCK2 domain has a single high affinity Ca^{2+} site, the Ca^{2+} bowl, defined by D897–901 (Schreiber and Salkoff, 1997; Bao et al., 2002, 2004). Neutralization of the negative-charged residues in these three sites abolishes the Ca^{2+}/Mg^{2+} sensitivity of BK channels comprised of α subunits (Bao et al., 2002; Shi et al., 2002; Xia et al., 2002). Positive-charged residues in the S4 segments together with other conserved charged residues in segments S2–S3 are associated with the voltage sensitivity in BK channels (Díaz et al., 1998;

C. Shelley and X. Niu contributed equally to this paper.
Correspondence to Karl L. Magleby: kmagleby@med.miami.edu
C. Shelley's present address is Dept. of Neuroscience, Physiology, and Pharmacology, University College London, London WC1E 6BT, England, UK.
X. Niu's present address is Center for Molecular Recognition, College of Physicians and Surgeons, Columbia University, New York, NY 10032.
Abbreviations used in this paper: MWC, Monod-Wyman-Changeux; SC, Schwarz criterion; wt, wild type.

The Rockefeller University Press $30.00
J. Gen. Physiol. Vol. 135 No. 5 461–480
www.jgp.org/cgi/doi/10.1085/jgp.200910331

Cui and Aldrich, 2000; Ma et al., 2006; Savalli et al., 2006). To a first approximation, the voltage sensors and high affinity Ca^{2+} sensors of BK channels function independently but synergistically to activate the channels (Cui and Aldrich, 2000; Rothberg and Magleby, 2000; Horrigan and Aldrich, 2002).

Extensive studies have shown that the voltage and high affinity Ca^{2+}_i-dependent gating of BK channels is consistent with a minimal two-tiered 50-state model with 25 closed states on the upper tier and 25 open states on the lower tier. The gating mechanisms developed in these previous studies are generally consistent with the macroscopic ionic and gating currents (Horrigan and Aldrich, 1999, 2002; Horrigan et al., 1999; Cui and Aldrich, 2000) and the single-channel kinetics (Rothberg and Magleby, 1998, 1999, 2000) over wide ranges of voltage and Ca^{2+}_i. Although these studies have proven highly useful toward understanding gating, there are still many unanswered questions. Both the macro current and single-channel studies assumed one high affinity Ca^{2+} binding site per subunit rather than the two known high affinity sites. The macro current studies typically focused on equilibrium constants rather than rate constants, so it is not necessarily clear whether it is the forward or backward (or both) rate constants that are altered by voltage and Ca^{2+}_i. The single-channel studies used models with limited numbers of states compared with the 50-state model, so it can be difficult to associate specific transitions in the simplified models with those in the 50-state model. Because all parameters were typically free in the models with limited numbers of states, it can be difficult to interpret the findings in terms of a consistent underlying structural mechanism.

Our present study addresses some of these questions for the voltage-dependent gating of BK channels. Single-channel recording and kinetic analysis is used to facilitate the determination of rate constants. Highly constrained models based on extensions of the Monod-Wyman-Changeux (MWC) model (Marks and Jones, 1992; Ríos et al., 1993; McCormack et al., 1994; Horrigan et al., 1999; Horrigan and Aldrich, 2002) are examined so that the data can be interpreted in terms of allosteric models based on the known quaternary structural features of BK channels. The determined rate constants allow the allosteric factors to be determined separately for forward and backward transitions. To activate the channel sufficiently (but not too much) so that single-channel data could be obtained over a wide range of negative and positive membrane potentials, the Mg^{2+} and RCK1 Ca^{2+} sensors were removed, leaving one Ca^{2+} bowl sensor on each subunit. Applying saturating Ca^{2+}_i then increased the activity sufficiently to obtain the required data and also forced the gating into mainly 10 of the 50 states, greatly simplifying the models and the determination of gating parameters.

We found for highly idealized 10-state two-tiered models and also for 15-state three-tiered models with a row of flicker states that the voltage sensors act mainly by decreasing the energy barrier for channel opening with little effect on the energy barrier for channel closing. Each additional activated voltage sensor increased the opening rate approximately an additional 23-fold while having little effect on the closing rate. In addition, we found that allowing cooperativity among the voltage sensors in these highly idealized models further improved the description of the gating, with each additional activated voltage sensor increasing the activation rate of the deactivated voltage sensors approximately fourfold. Whether this apparent cooperativity arises from imposing highly idealized models or represents actual cooperativity will require additional studies to resolve. The highly idealized gating mechanisms could describe the single-channel kinetics over wide ranges of voltage and will provide tools to relate kinetics to underlying structure.

MATERIALS AND METHODS

Clones, mutagenesis, and channel expression

Experiments were performed using the mouse Slo1 α subunit of the BK channel (Butler et al., 1993) as modified by Xia et al. (2002) to disable the RCK1 high affinity Ca^{2+} sensor (D362A/D367A) and the low affinity Ca^{2+}/Mg^{2+} sensor (E399A), leaving the Ca^{2+} bowl sensor. The channels were transiently expressed in HEK293 cells together with green fluorescent protein to identify transfected cells as described previously (Nimigean and Magleby, 1999). In a few experiments, when specifically indicated, the mutated channels were expressed in *Xenopus laevis* oocytes after injection of cRNA as described previously (Qian et al., 2006).

Electrophysiology and solutions

Single-channel currents were recorded from excised inside-out patches of membrane using Axopatch 200A or 200B amplifiers (Molecular Devices). Data were obtained from patches containing a single channel, which was verified by increasing Po to >0.5 and observing a single open current level for extend periods of recording. The pipette solution contained 150 mM KCl and 5 mM TES buffer. The solution at the intracellular side of the excised patches of membrane contained 150 mM KCl, 5 mM TES, 1 mM EGTA, and 1 mM HEDTA. In addition, 50 μM 8-crown ether ((+)-18-Crown-6)-2,3,11,12-tetracarboxylic acid was included in the intracellular solution in most experiments to bind contaminant Ba^{2+} to prevent occasional long channel blocks (Diaz et al., 1996; Bello and Magleby, 1998). In addition to binding Ba^{2+} (dissociation constant of 1.6×10^{-10} M), 18-crown ether also binds K^+ (3.3×10^{-6} M) and Ca^{2+} (10^{-8} M; Diaz et al., 1996). Sufficient Ca^{2+} was added to the solutions to obtain free Ca^{2+} of either 95 or 283 μM, as calculated with an in-house buffer program. Unless indicated otherwise, experiments were performed with 95 μM intracellular free (Ca^{2+}_i). Solutions were adjusted to pH 7.0. Recordings were made at room temperature (22–25°C).

Estimating rate constants and gating parameters for kinetic models

The methods for using 50% threshold analysis to measure open- and closed-interval durations, identifying stable single-channel data with stability plots, plotting 1-D and 2-D dwell-time

distributions, applying maximum likelihood methods to describe 1-D dwell-time distributions with sums of exponentials, and estimating the most likely rate constants and gating parameters from simultaneous (global) maximum likelihood fitting of 2-D dwell-time distributions obtained over a range of experimental conditions (in this case voltage) have been described in detail previously (McManus and Magleby, 1988; Rothberg and Magleby, 2000; Gil et al., 2001). Missed events were taken into account when estimating the gating parameters using the method described by Crouzy and Sigworth (1990).

Ranking kinetic models

Two methods were used to rank the different kinetic schemes: the likelihood ratio test and the Schwarz criterion (SC). The likelihood ratio test applies to nested models and provides both a ranking and a significance for the ranking (Horn and Lange, 1983). The models examined in this study are nested because the simpler schemes are contained in the more complex schemes. The SC (also referred to as the Schwarz information criterion or the Bayesian information criterion) applies to both nested and nonnested models and provides ranking but not the significance of the ranking (Koehler and Murphree, 1988).

Adding additional free gating parameters to a model typically increases the likelihood of the fit. To determine whether the fit is significantly better using the likelihood ratio test, the models were compared by determining the LLR_k from $LLR_k = LL_k - LL_{k\text{-}n}$, where LLR_k is the natural logarithm of the ratio of the maximum likelihoods for k versus k-n free parameters, and LL_k and $LL_{k\text{-}n}$ are the natural logarithms of the maximum likelihoods that the experimental data were drawn from the 2-D dwell-time distributions predicted by the models with the indicated number of free parameters. Twice the value of LLR_k is distributed as χ^2, with the degrees of freedom equal to n, the difference in the number of free parameters. For example, a model with two additional free parameters is judged significantly better ($P < 0.05$) when the LLR_k is >2.996, as two times this value is 5.99, the χ^2 value for two degrees of freedom at the 0.05 level (Horn and Lange, 1983). A table for determining significance with the likelihood ratio test is found in Rothberg et al. (1997). Note that the likelihood values take the number of analyzed intervals into consideration, as the log likelihood values for a given model (for perfect data) are directly proportional to the number of analyzed intervals.

The SC is given by $SC = -LL + (0.5\ F)\ \ln N$, where LL is the natural logarithm of the maximum likelihood estimate, F is the number of free parameters, and N is the number of intervals. The scheme with the smallest SC is ranked first. As an example, for N = 36,000 interval pairs, adding two additional free gating parameters to a model needs to increase the LL by >10.49 for the more complex model to be ranked first. In contrast, with the likelihood ratio test, a model with two additional free parameters needs to increase the LL by >2.996 for the more complex model to be ranked significantly better. Thus, for 36,000 open–closed-interval pairs obtained over a range of voltages, the SC has an approximately threefold greater penalty for additional free parameters. The number of interval pairs that were simultaneously fitted for each channel was 42,147 DM1, 28,738 DM2, 34,100 DM3, and 38,376 DM4.

The maximum likelihood values determined during the fitting are useful for ranking models but give little information about how well the considered models actually describe the dwell-time distributions. To obtain a quantitative comparison of the ability of various models to describe the data when compared with the highest ranking model, the normalized likelihood ratio per interval pair, NLR_1, was calculated from $NLR_1 = \exp([LL - LL_H]/N)$, where LL and LL_H are the natural logarithms of the likelihoods for the model under consideration and the highest ranked model, respectively, and N is the number of interval pairs in the fitted 2-D dwell-time distributions (Gil et al., 2001). An NLR_1 of 1.0 indicates that the two compared models give equally likely descriptions of the data. An NLR_1 of 0.9 indicates the likelihood that an interval pair drawn from the 2-D distributions predicted by the model under consideration is only ~90% of the likelihood for the top-ranked model. Values are expressed as the mean ± SEM.

Online supplemental material

Tables S1 and S2 present the exponential components that describe the open and closed dwell-time distributions, respectively, for the various examined channels and voltages. These tables quantify the effect of voltage on the shifts in the distributions. For evaluation of kinetic schemes, 2-D dwell-time histograms (see example in Fig. 6 A) obtained over a wide range of voltages were simultaneously fitted. Table S3 presents the gating parameters for one channel, DM4. Table S4 gives the various schemes, number of free parameters, log likelihoods, and ranking by the likelihood ratio test for various schemes for each channel. Table S5 presents the SC ranking for three different pairs of kinetic schemes for each of the four channels. Online supplemental material is available at http://www.jgp.org/cgi/content/full/jgp.200910331/DC1.

RESULTS

Single-channel analysis was used to characterize the allosteric coupling and cooperative factors involved in activation of BK channels by voltage. Coupling in this study refers to the action of the voltage sensors on altering the transition rates for opening and closing. Cooperativity refers to interactions among the voltage sensors. Coupling and cooperativity will be specifically defined in terms of kinetic models to be presented later.

BK_B channels in saturating Ca^{2+}_i simplify the gating mechanism and shift the Po versus voltage curve into a useable range to obtain single-channel data

Because of the extremely low activity of BK channels at negative potentials in the absence of Ca^{2+}_i, it can be difficult to obtain sufficient single-channel data for analysis. Consequently, we took advantage of the synergistic activation of BK channels by voltage and Ca^{2+}_i (Barrett et al., 1982; Cui et al., 1997), using Ca^{2+}_i to left shift the Po versus voltage curves so that sufficient single-channel data could be obtained over a wide range of both negative and positive potentials. To simplify the gating mechanism, the experiments were performed in saturating Ca^{2+}_i on modified BK channels, termed BK_B channels, mutated to have a single Ca^{2+} sensor per subunit, the Ca^{2+} bowl. Saturating Ca^{2+}_i was used to drive the channel into a reduced number of states, as will be explained in a later section. A single Ca^{2+} sensor per subunit was used to reduce the numbers of potential states and to shift the gating into a voltage range in which the full range of open probability, Po, could be studied using potentials between ±100 mV, where the membrane remains stable.

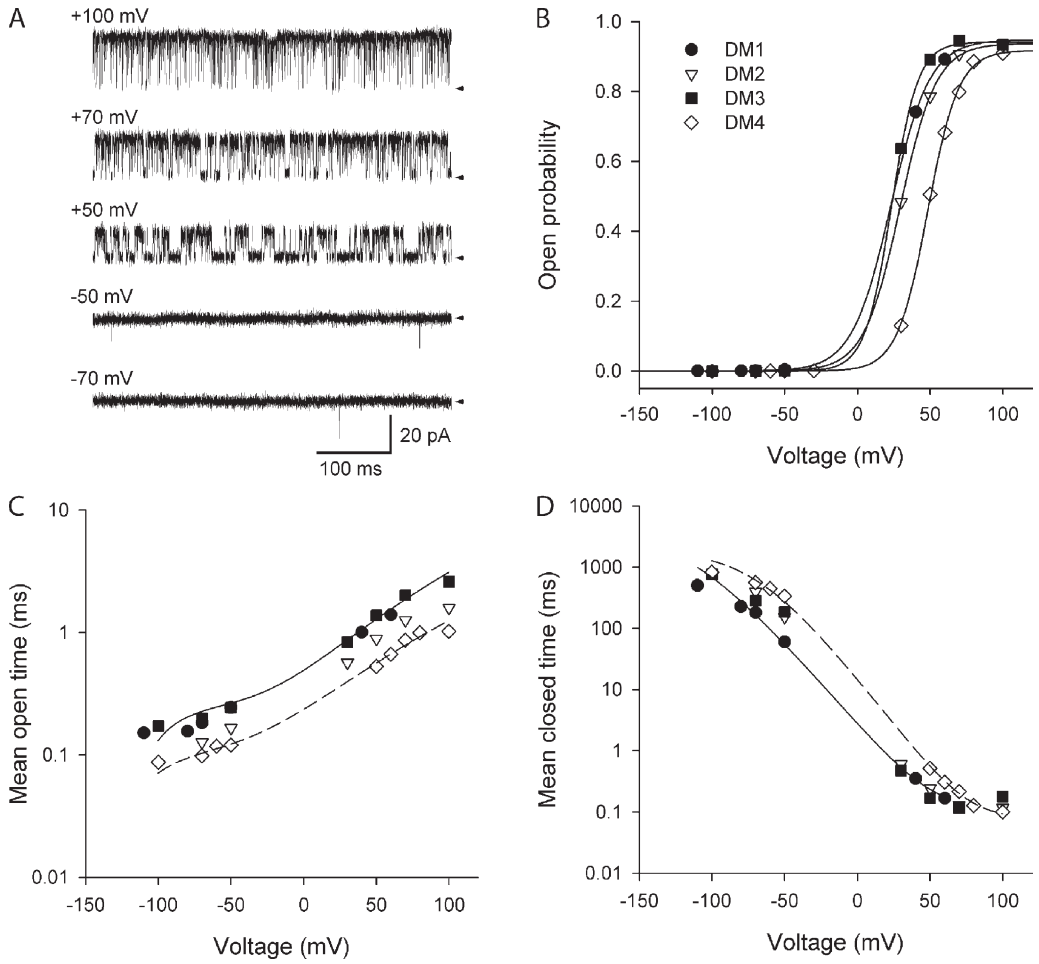

Figure 1. Voltage activation of BK_B channels. (A) Representative single-channel currents recorded from a BK_B channel (DM4) in saturating 95 µM Ca^{2+}_i. Arrows indicate the closed channel levels. (B) Plots of Po versus voltage for four separate BK_B channels, as indicated. The lines are fits with the Boltzmann equation $Po = Po_{max}/(1 + \exp[(V_{0.5} - V)/b])$, where b is the voltage sensitivity expressed as the voltage change (in millivolts) per e-fold change in Po. The parameters for the lines are given in Table I. (C and D) Voltage dependence of mean open and mean closed times for the same four channels as in B. The lines plot the predicted mean open and closed times for channels DM1 (continuous lines) and DM4 (dashed lines) calculated with Scheme V. A similar superposition of observed and predicted mean open and mean closed times was observed for channels DM2 and DM3. Parameters used in the predictions for channel DM4 in C and D of this figure and in Figs. 4–7 are given in Table S3.

To construct the BK_B channels, the high affinity RCK1 Ca^{2+} sensor and the low affinity Ca^{2+}/Mg^{2+} sensor on each subunit were disabled with the mutations D362A/D367A and E399A, respectively (Xia et al., 2002; Zeng et al., 2005). To assure saturating activation of the remaining Ca-bowl sensors, all experiments were performed with 95 µM free Ca^{2+}_i, which is >20-fold greater than the apparent K_d for the Ca bowl

TABLE I

Voltage dependence of individual BK_B channels

Channel	V0.5	Millivolts per e-fold change in Po[a]	q_G (e_o)[b]	Po_{max}
	mV			
DM1	22.9	13.4	1.90	0.95
DM2	29.0	12.5	2.04	0.94
DM3	23.0	9.1	2.80	0.94
DM4	48.0	10.6	2.41	0.92
Mean	30.7 ± 5.9	11.4 ± 1.0	2.29 ± 0.20	0.94 ± 0.1

The means ± SEM are presented in the bottom row.

[a]The voltage sensitivity is defined as the voltage change (in millivolts) required for an e-fold change in Po.

[b]Effective gating charge $q_G = k_BT/$(millivolts per e-fold change in Po), where k_B is Boltzmann's constant, T is absolute temperature, and k_BT = 25.5 (millivolts e_o) at 23°C.

(Bao et al., 2002; Xia et al., 2002). Observations consistent with saturation of Ca-bowl sites with ~100 μM Ca^{2+}_i have been reported previously (Rothberg and Magleby, 1999; Bao et al., 2002; Xia et al., 2002). As a further test of saturation, we found no significant difference in Po for BK_B channels with 95 and 283 μM free Ca^{2+}_i at −100 mV (0.00021 ± 0.00008 vs. 0.00020 ± 0.00007, P > 0.9, n = 3–5) for experiments with single-channel recording.

Voltage dependence of BK_B channels in saturating Ca^{2+}_i

Single-channel currents from a BK_B channel are shown in Fig. 1 for voltages ranging from −70 to 100 mV with 95 μM of saturating free Ca^{2+}_i. Similar to wild-type (wt) BK channels, depolarization activates BK_B channels, increasing channel activity, as indicated previously (Xia et al., 2002). The voltage-dependent increase in Po is plotted in Fig. 1 B for four BK_B channels, each studied separately in a single-channel patch. Each channel has the same general activation response, but individual channels have somewhat different values for $V_{0.5}$, the voltage for half activation. Such variability among individual channels and even among macro currents recorded from different patches containing large numbers of channels is observed for BK channels (McManus and Magleby, 1991; Rothberg and Magleby, 1998; Horrigan and Aldrich, 2002; Niu and Magleby, 2002). Fitting the data from each channel with a single Boltzmann distribution gives the values in Table I, with a mean $V_{0.5}$ of 30.7 ± 5.9 mV (SEM), a mean slope of 11.4 ± 1.0 mV/e-fold change in Po, an effective partial charge movement for activation of 2.29 electronic units (e_o), and a maximum Po of 0.94 ± 0.01. The voltage sensitivity (slope) for these BK_B channels agrees with that observed previously for native BK channels in cultured rat skeletal muscle of 11.1 ± 3.1 mV (Rothberg and Magleby, 2000). The effective partial charge over the voltage range of these experiments of 2.29 e_o is consistent with previous single-channel (Rothberg and Magleby, 2000), ionic (Horrigan et al., 1999; Ma et al., 2006), and gating current (Horrigan and Aldrich, 1999, 2002) studies for wt BK channels. Therefore, the mutations to disable the RCK1 Ca^{2+} sensors and the low affinity Ca^{2+}/Mg^{2+} sensors appear to have little, if any, effect on the voltage activation mechanism.

Fig. 1 (C and D) shows that the increase in Po with depolarization in BK_B channels arises from changes in both the open- and closed-interval durations. Depolarizing from −100 to 100 mV increased the mean open time ~12-fold from 0.14 to 1.7 ms and decreased mean closed time ~4,500-fold from 580 to 0.13 ms. Such depolarization-induced changes in mean open and closed intervals, with the dominant effect on the closed intervals, are also a characteristic of wt BK channels (Rothberg and Magleby, 2000).

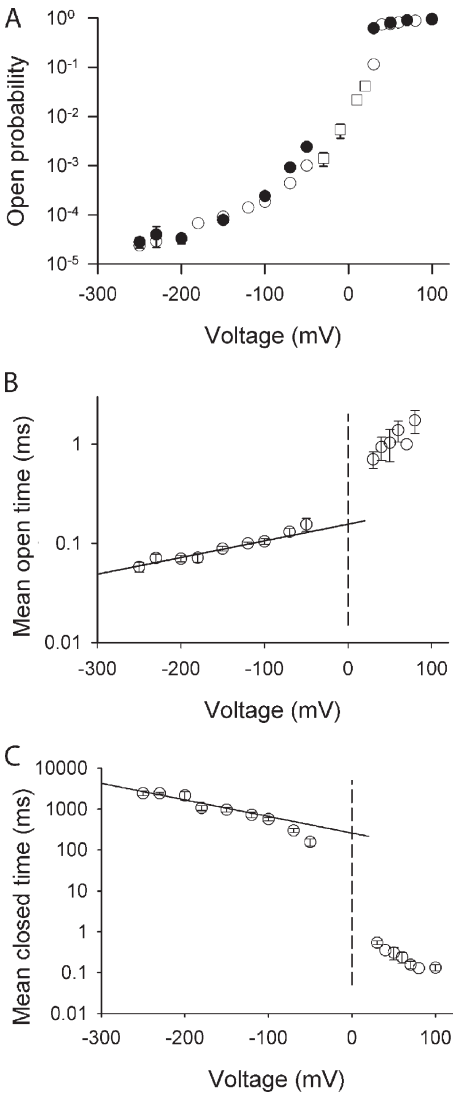

Figure 2. Estimating the partial charge associated with the opening and closing transitions for BK_B channels gating in saturating Ca^{2+}_i. (A) Plot of Po versus voltage. Circles plot data obtained for BK_B channels expressed in oocytes for patches with a single channel (open circles) and from two to six channels per patch (closed circles). Squares plot data obtained from macro currents from BK_B channels expressed in HEK cells. (B) Voltage dependence of mean open times at negative potentials. The line is a linear fit to open times negative to −100 mV. Projecting to 0 mV gives an intrinsic channel closing rate (K in Schemes III, IV, and V) of 6,420 ± 680 s^{-1} with a partial charge of −0.099 ± 0.015 e_o (257 mV/e-fold change). (C) Voltage dependence of mean closed times. The line is a linear fit to closed times negative to −100 mV. Projecting to 0 mV gives an estimate of the intrinsic opening rate (H in Schemes III, IV, and V) of 3.87 ± 1.88 s^{-1} with a partial charge of 0.237 ± 0.06 e_o (108 mV/e-fold change). Data in B and C are a mean of the data obtained with single-channel recording.

Voltage dependence of the opening and closing transitions

The voltage dependence of the gating of wt BK channels, and also presumably for the mutant BK_B channels because of their essentially identical voltage sensitivity to wt channels (see preceding section), reflects gating

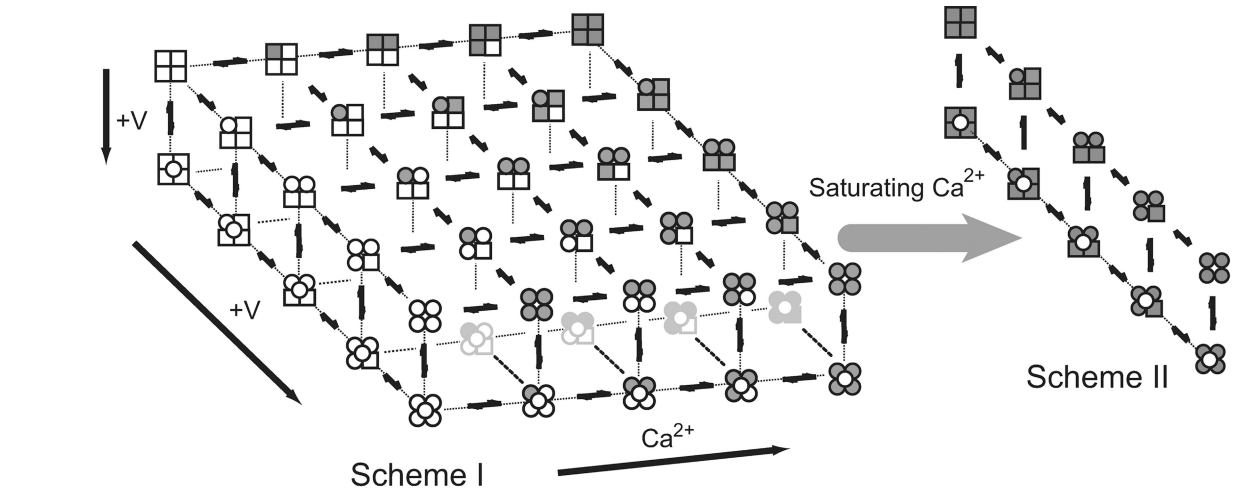

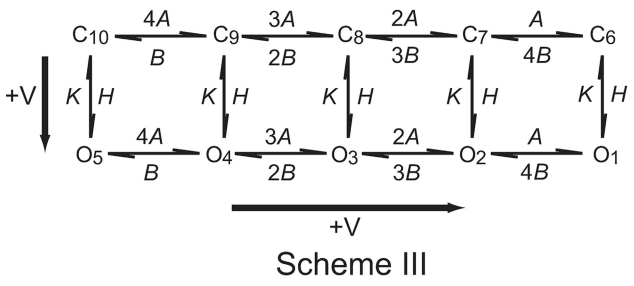

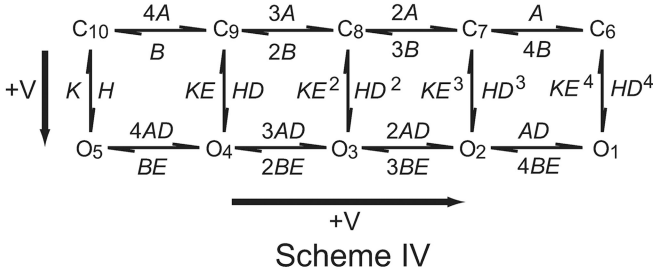

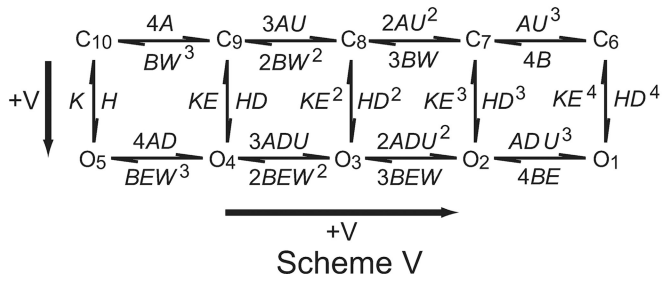

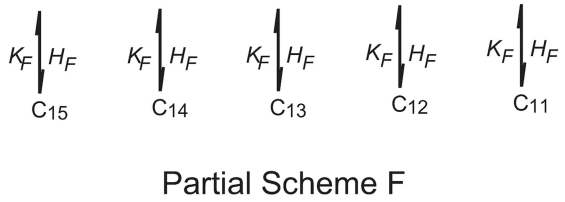

charge movement associated mainly with the voltage-dependent movement of the S4 voltage sensors and also a weaker voltage dependence associated with the opening/closing transitions (Díaz et al., 1998; Horrigan et al., 1999; Rothberg and Magleby, 2000; Horrigan and Aldrich, 2002; Ma et al., 2006). At very negative potentials the voltage dependence of the opening/closing transitions can be estimated directly because the S4 voltage sensors are held in their resting positions (Stefani et al., 1997; Horrigan et al., 1999; Horrigan and Aldrich, 2002). Fig. 2 A plots Po versus voltage for data obtained from patches with one or more BK_B channels at saturating (95 μM) Ca^{2+}_i. The shallow part of the curve at voltages more negative than approximately −100 mV reflects the voltage dependence of the opening and closing transitions, as the S4 voltage sensors are held in their deactivated positions. The steeper part of the curve reflects mainly the voltage dependence of the movement of the S4 voltage sensors as well as the voltage dependence of the opening and closing transitions (Horrigan and Aldrich, 2002; Ma et al., 2006).

Fig. 2 (B and C) plots the mean open time and mean closed time versus voltage. Fitting the voltage dependence of the mean open and closed times at voltages more negative than −100 mV indicates a partial charge of -0.0994 ± 0.015 e_o for the closing transition (−257 mV per e-fold increase in closing rate) with a projected rate constant of $6{,}420 \pm 680$ s^{-1} at 0 mV (Fig. 2 B) and a partial charge of 0.237 ± 0.06 e_o for the opening transition (108 mV per e-fold increase in opening rate) with a projected rate constant of 3.87 ± 1.88 s^{-1} at 0 mV (Fig. 2 C). These estimates of partial charge are not significantly different from the estimates of -0.145 ± 0.007 e_o for the closing transitions ($P > 0.1$) and 0.22 ± 0.005 e_o for the opening transition ($P > 0.7$) obtained by Horrigan and Aldrich (2002) for wt BK channels with 70–100 μM Ca^{2+}_i. Estimates of partial charge movement from Rothberg and Magleby (2000) for the C-O and

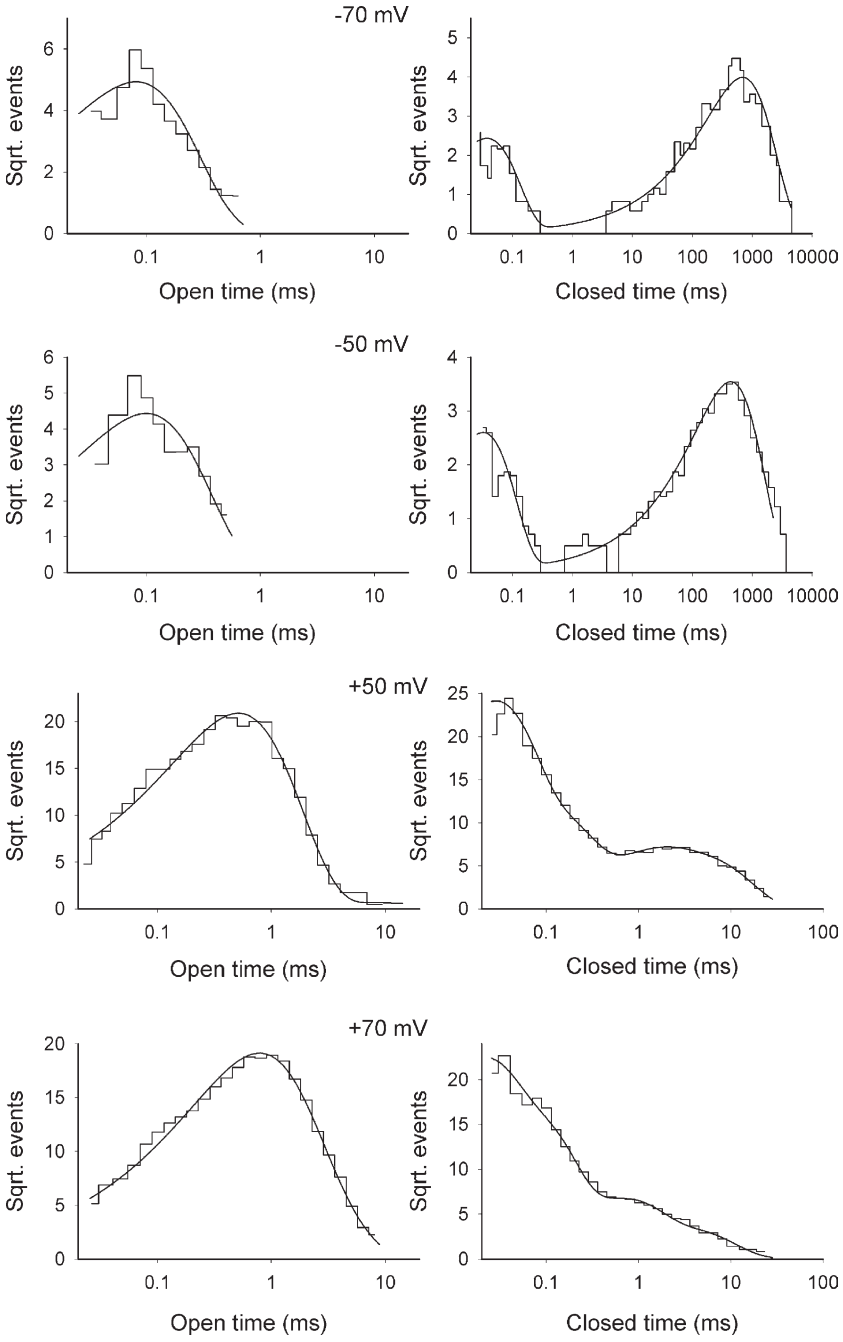

Figure 3. Open and closed dwell-time distributions for BK_B channel DM4 at the indicated voltages in saturating Ca^{2+}_i. Lines are mixtures of exponential components fitted to the dwell times. Open time histograms were described by one to two significant exponential components, and closed time histograms were described by two to five significant exponential components. The time constants and areas of the exponentials for the four studied channels are given in Tables S1 and S2. A moving bin mean of three consecutive bins was used for the data at negative potentials because of the small numbers of intervals at the low Po. Channel DM4 is presented in Figs. 3–7 as a representative channel. Similar conclusions were reached with channels DM1–DM3.

O-C transitions are also, within experimental variability, consistent with the aforementioned two estimates.

Dwell-time distributions for BK_B channels in saturating Ca^{2+}_i

Fig. 3 plots representative open and closed dwell-time distributions obtained from a BK_B channel at −70, −50, 50, and 70 mV with saturating 95 µM Ca^{2+}_i. For this channel and the three additional channels studied in detail, the open and closed distributions were typically described by the sums of two open exponential components and three to five closed exponential components, respectively, similar to wt BK channels for a similar number of analyzed intervals (McManus and Magleby, 1988; Rothberg and Magleby, 2000). Therefore, BK_B channels are predominantly gating in a minimum of two open and three to five closed states for each voltage.

Exploring the voltage-dependent gating mechanisms for BK_B channels using highly idealized constrained models

Scheme I presents a 50-state two-tiered model as a possible gating mechanism for a channel with one Ca^{2+} sensor and one voltage sensor per subunit (for review see Magleby, 2003), as is the case for the BK_B channel. Adding sufficient Ca^{2+}_i to saturate the Ca^{2+} bowl for the BK_B channel would then effectively drive the gating to

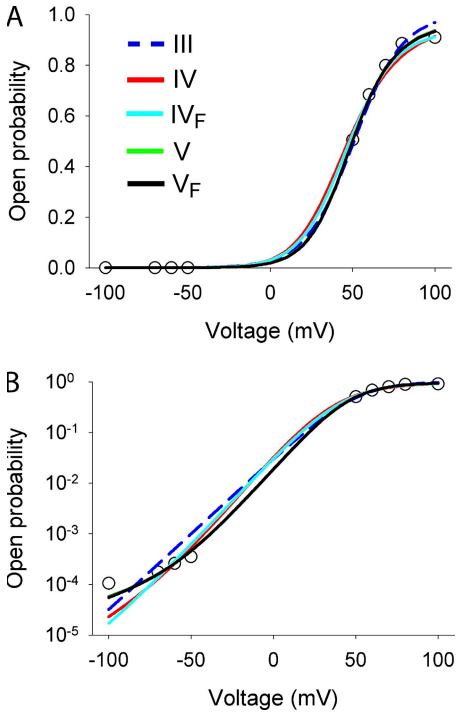

Figure 4. Comparison of the observed and predicted voltage dependence of Po for BK_B channel DM4 on linear and log-linear coordinates for the indicated gating mechanisms with saturating Ca^{2+}_i. Open circles, observed voltage dependence; lines, predicted voltage dependence. A, linear coordinates; B, log-linear coordinates. Saturating Ca^{2+}_i. The predictions of Schemes V and V_F (green and black lines) superimpose over most of the voltage range and give a somewhat more accurate description of the data at negative voltages than the other schemes.

the right-most 10 states, giving the 10-state model indicated by Scheme II. Previous studies have shown that voltage and Ca^{2+} activation of wt BK channels can be approximated by Scheme I and that voltage activation alone can be approximated by Scheme II (Cox et al., 1997; Horrigan and Aldrich, 1999, 2002; Rothberg and Magleby, 1999, 2000; Horrigan et al., 1999; Cui and Aldrich, 2000; Bao et al., 2002; Ma et al., 2006; for review see Magleby, 2003).

We now expand on Scheme II to examine the specific allosteric coupling and cooperative factors involved in the gating of BK_B channels by voltage for the 10-state model induced by saturating Ca^{2+}. The models to be tested are indicated by Schemes III–V with the indicated constraints on the gating parameters. These idealized schemes are based on previous constrained models for various voltage-dependent channels (Marks and Jones, 1992; Ríos et al., 1993; McCormack et al., 1994) and also for wt BK channels (Cox et al., 1997; Horrigan and Aldrich, 1999, 2002; Horrigan et al., 1999; Ma et al., 2006). These schemes can also be considered as extensions of models for BK channels with a limited number of states with unconstrained rate constants (Rothberg and Magleby, 1998, 1999, 2000).

The gating parameter A in these schemes is the forward rate constant for the activation of a single voltage sensor at 0 mV. B is the backward rate constant for deactivation of a voltage sensor at 0 mV. The 4, 3, 2, and 1 for the forward activation and backward deactivation of voltage sensors indicate the number of voltage sensors available for activation or deactivation, respectively. H and K are the opening and closing rate constants when all voltage sensors are deactivated, and H_F and K_F are the rate constants to and from flicker closed states. Partial Scheme F is an additional tier of closed states that can be added below any of the above schemes to add a tier of brief flicker closed states that are entered from the open states.

A, B, H, and K have allowed voltage dependence, with the voltage dependence described by $\text{Rate}(V) = \text{Rate}(0)\exp(Vq/kT)$, where q is the effective charge movement associated with the transition. For an effective charge of 1.0 e_o for q, $q/kT = 1/25.5$ mV at 23°C. D and E in Schemes IV and V are coupling factors for channel opening and closing, where each activated voltage sensor changes the opening rate D-fold and the closing rate E-fold. Thus, one to four activated voltage sensors change the opening rates by D, D^2, D^3, and D^4 and the closing rates by E, E^2, E^3, and E^4. U and W in Scheme V are cooperative factors for voltage sensor activation and deactivation, respectively. Each activated voltage sensor changes the activation rate of each of the deactivated voltage sensors U-fold, and each deactivated voltage sensor changes the deactivation rate of each of the activated voltage sensors W-fold. Therefore, one to three activated voltage sensors would increase the activation rate of the deactivated voltage sensors by U, U^2, and U^3, and one to three deactivated voltage sensors would change the deactivation rate of the activated voltage sensors by W, W^2, and W^3. Values of D, E, U, and W>1.0 would increase transition rates, and values <1.0 would decrease transition rates.

Schemes III–V depict only a few of the many possible mechanisms that could be proposed for gating. Although it seems unlikely that gating would exactly follow such a systematic imposition of the effects of one to four activated voltage sensors on coupling and cooperativity, these highly constrained idealized models can serve as useful starting points for analysis. Notice that with the exception of A and B, these parameters have different meanings than those in Horrigan and Aldrich (2002).

Because the gating of BK channels is consistent with microscopic reversibility (McManus and Magleby, 1989; Song and Magleby, 1994), the rate constants in Schemes III–V are further constrained so that the transitions around any of the 10 possible loops in these schemes are identical in the clockwise and counterclockwise directions (Colquhoun and Hawkes, 1995). Imposing microscopic reversibility requires the inclusion of D and E in

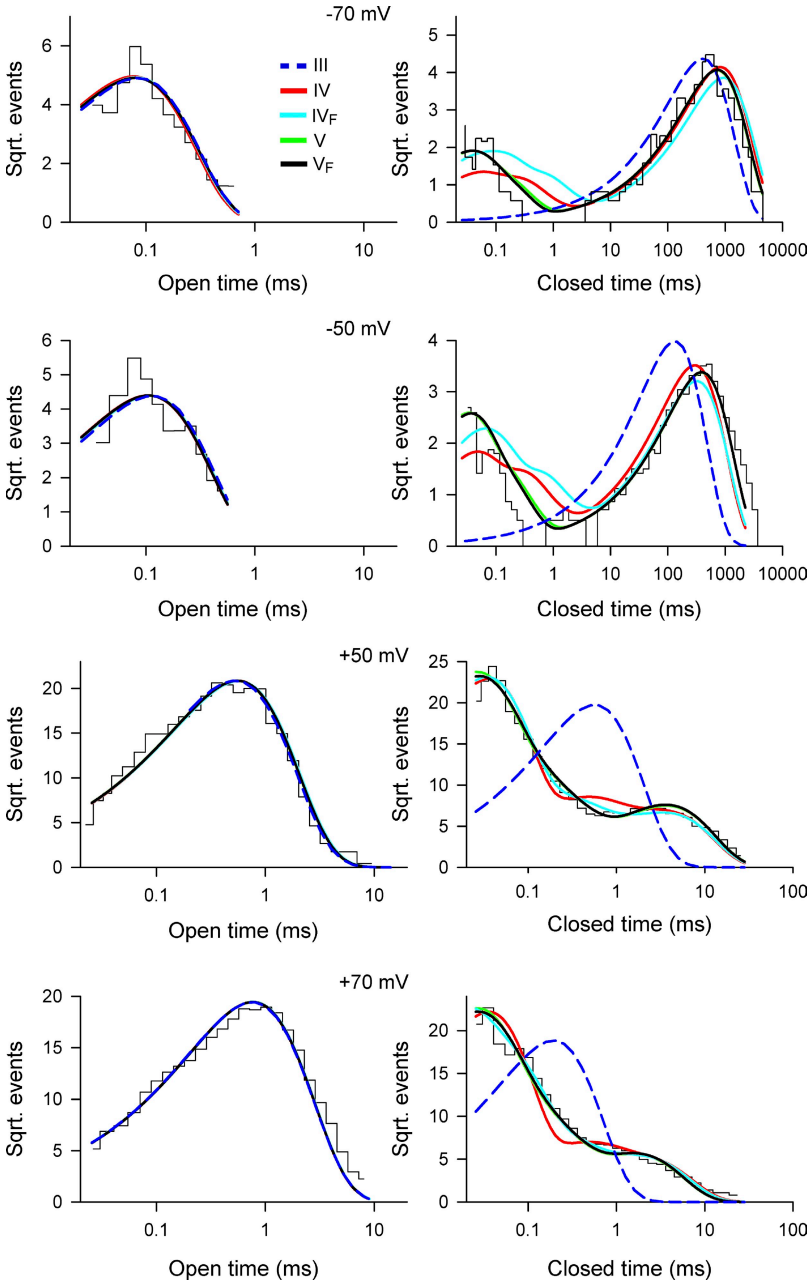

Figure 5. Open and closed dwell-time histograms for BK_B channel DM4 obtained at the indicated voltages with saturating Ca^{2+}_i overlaid with the distributions predicted by the indicated kinetic schemes. Although all four schemes predicted the voltage-dependent shifts in the open dwell-time histograms, only Schemes V and V_F could predict the voltage dependence of the closed dwell-time histograms over the entire voltage range.

specifying the transition rates between the open states in Schemes IV and V.

Scheme III approximates Po over limited voltage ranges, accounts for the voltage dependence of the open dwell times, and does not describe the closed dwell times

We first examined whether Scheme III, which has no coupling or cooperative factors, could describe the voltage-dependent gating of BK_B channels. This was done by simultaneously fitting 2-D dwell-time distributions of adjacent open and closed intervals obtained at six to nine different voltages with Scheme III to obtain the values for the rate constants *A*, *B*, *K*, and *H* that maximized the probability that the single-channel data were drawn from the 2-D distributions predicted by Scheme III. The most likely rate constants determined from fitting were then used with Scheme III to predict Po and the dwell-time distributions for comparison to the experimental data.

Fig. 4 (A and B) presents linear and log-linear plots showing that Scheme III can approximate the large increases in Po with depolarization but gives a poor description of Po for negative voltages (dashed blue lines). Scheme III can describe the depolarization-induced right shift to longer open times in the open dwell-time distributions (Fig. 5, left, dashed blue lines). However, Scheme III could not describe the voltage dependence of the closed dwell-time distributions (Fig. 5, right, dashed blue lines). The most likely parameters for Scheme III for channel DM4 are in Table S3, where

TABLE II

SC ranking and normalized likelihood ratios for individual BK_B channels

Scheme	Free parameters[a]	SC ranking				Normalized likelihood ratio			
		DM1	DM2	DM3	DM4	DM1	DM2	DM3	DM4
III	8	5	5	5	5	0.380	0.224	0.130	0.345
IV	10	4	4	4	4	0.964	0.944	0.921	0.979
IV_F	12	3	3	3	2	0.985	0.980	0.944	0.999
V	12	2	2	2	3	0.998	0.998	0.995	0.998
V_F	14	1	1	1	1	1.000	1.000	1.000	1.000

[a]The number of free parameters for channel DM3 is two less than indicated because $q_H = 0.237$ e_o and $q_K = -0.0994$ e_o were fixed to values determined from Fig. 2.

it can be seen that depolarization increases *A*, the rate constant for voltage sensor activation, through q_A (0.0721 e_o), decreases *B*, the rate of voltage sensor deactivation, through q_B (−0.100 e_o), increases the opening rate constant *H* through q_H (1.36 e_o), and decreases the closing rate constant *K* through q_K (−0.383 e_o). These most likely (in terms of the model) indirect estimates of partial charge for Scheme III place the majority of the voltage dependence in the opening and closing transitions rather than in voltage sensor activation and deactivation, the opposite of what is observed with more direct measurements (Horrigan and Aldrich, 1999; Horrigan et al., 1999) or more likely models (see following paragraph and Rothberg and Magleby, 2000). The complete inability of Scheme III to account for the closed dwell-time distributions (Fig. 5, right, dashed blue lines) requires that this scheme be rejected and suggests that additional factors are involved in the gating of BK_B channels.

Schemes IV and V give progressively improved descriptions of the single-channel kinetics

We next examined whether Scheme IV, with the added allosteric parameters *D* and *E* to couple the opening and closing transitions to the voltage sensor movement, could describe the single-channel kinetics. Scheme IV approximated the increase in Po with depolarization (Fig. 4, red lines) and described the right shift in the open dwell-time distributions with depolarization (Fig. 5, left, red lines). Scheme IV gave a greatly improved description of the closed distributions compared with Scheme III, but there were still some marked differences between the observed and predicted distributions (Fig. 5, right, red lines).

We next examined whether Scheme V, which is like Scheme IV but with allowed cooperativity among the voltage sensors through the parameters *U* and *W*, would improve the description of the data over Scheme IV. Scheme V gave a somewhat improved description of the effect of depolarization on Po (Fig. 4, green lines often masked by black lines) and described the effect of depolarization on the open dwell-time distributions (Fig. 5, left, green lines often masked by black lines). Scheme V also gave further improved descriptions of the closed dwell-time distributions over Scheme IV, capturing all the major features (Fig. 5, right, green lines often masked by black lines).

Adding flicker closed states improves the description of the single-channel kinetics

Rothberg and Magleby (1998, 1999) found for simplified gating mechanisms for wt BK channels that the addition of a brief closed state to each open state to generate additional brief closed intervals (flickers) improved the ability of the models to describe the experimental data. Consequently, we examined whether the addition of partial Scheme F to Schemes IV and V to add a flicker state to each open state would improve the description of the data. The addition of flicker states to Scheme IV to form Scheme IV_F had little effect on the descriptions of Po and the open distributions but gave improved descriptions of the closed dwell times except for very brief intervals at negative potentials (compare blue continuous lines with the red lines in Figs. 4 and 5, right). The addition of flicker states to Scheme V to form Scheme V_F gave essentially the same excellent visual description of the data as Scheme V (Figs. 4 and 5, black lines superimposing the green lines). Thus, Schemes V and V_F, both of which have coupling and cooperativity, describe the voltage dependence of Po and the single-channel kinetics.

Ranking the different gating mechanisms

Table II ranks the various schemes for the four different examined channels on the basis of likelihood using the SC, which applies a heavy penalty for additional free parameters (see Materials and methods). For channels DM1, DM2, and DM3, the ranking of the various schemes was, from lowest to highest, Schemes III, IV, IV_F, V, and V_F. The rankings were the same for channel DM4 except that the rankings of Schemes IV_F and V were reversed. The likelihood ratio test (see Materials and methods) gave the same rankings as the SC and also indicated that each of the higher ranked models were significantly better than the lower ranked models ($P < 0.001$; Table S4). The top-ranked Scheme V_F had both

coupling (*D* and *E*) and cooperative factors (*U* and *W*) as well as flicker closed states.

Also listed in Table II are the normalized likelihoods per interval pair for each of the schemes and channels expressed as a ratio to the top-ranked Scheme V_F (see Materials and methods). Averaging the normalized likelihood ratios in Table II for the four channels indicated that Schemes III, IV, IV_F, and V were 0.270, 0.952, 0.977, and 0.997 as likely, respectively, per interval pair as the top-ranked Scheme V_F.

Predicting the 2-D dwell-time distributions and single-channel currents

Fig. 6 shows that the top-ranked Scheme V_F can approximate the description of the 2-D dwell-time distributions. These distributions include the information in the 1-D distributions, as in Fig. 5, as well as correlation information that helps define the connections among states (Fredkin et al., 1985; Magleby and Song, 1992; Gil et al., 2001). Fig. 6 A presents a 2-D dwell-time distribution of experimental data for gating at 50 mV. The distribution plots the square root of the number of observed adjacent interval pairs in each bin on the z axis versus the log of the mean open- (y axis) and closed (x axis)-interval durations for that bin. The interpretation of such plots has been presented previously in detail (Magleby and Song, 1992; Rothberg and Magleby, 1998) so will only be described here in brief. Fig. 6 A indicates that the most frequently observed interval pairs for BK_B channels at 50 mV with saturating Ca^{2+}_i are longer openings adjacent to briefer closings, as indicated by the prominent peak at −0.5 (0.3 ms) on the y axis and −1.5 (0.03 ms) on the x axis. Three additional frequently observed adjacent interval pairs are present in Fig. 6: longer openings adjacent to longer closings (bump in right back quadrant of plot), shorter openings adjacent to longer closings (bump in right front quadrant), and briefer openings adjacent to briefer closings (bump in left front quadrant). A visual comparison of the experimental distribution in Fig. 6 A to the predicted distribution in Fig. 6 B shows that Scheme V captures the major features of the 2-D dwell-time distribution.

Fig. 7 presents simulated single-channel currents for Scheme V for comparison with the experimental currents in Fig. 1 A. The major features of the single-channel currents are captured by Scheme V over the wide range of voltages examined.

Gating parameters for Schemes IV, IV_F, V, and V_F

Table III presents the estimated gating parameters for Schemes IV through V_F as the mean ± SEM of the estimates for each of the four examined channels. Table S3 presents the parameters for channel DM4 for Schemes III through V_F. In interpreting the parameters, it needs to be kept in mind that the examined schemes are

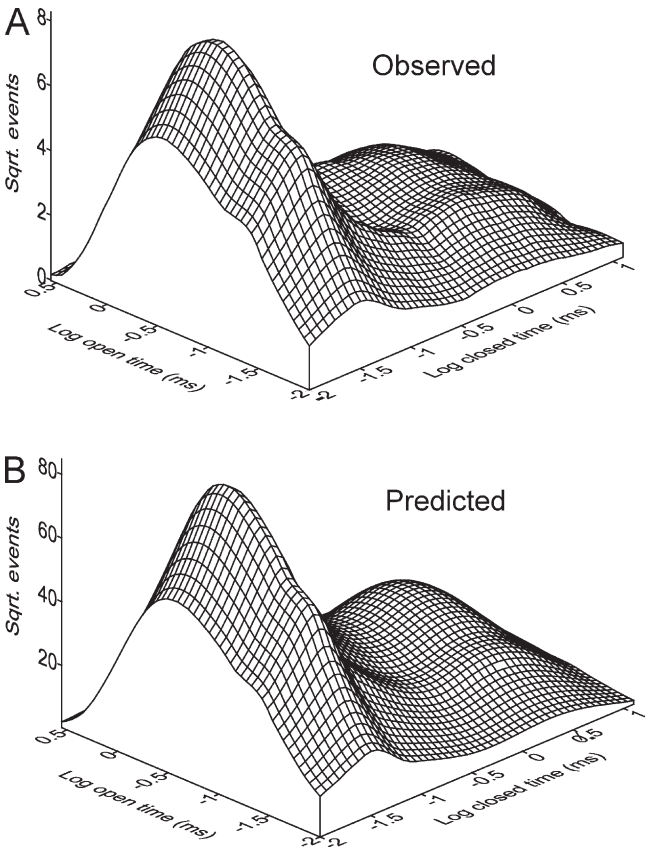

Figure 6. Observed and predicted 2-D dwell-time distributions of open–closed- and closed–open-interval pairs for Scheme V for BK_B channel DM4 at 50 mV with saturating Ca^{2+}_i. Scheme V approximated the 2-D distributions.

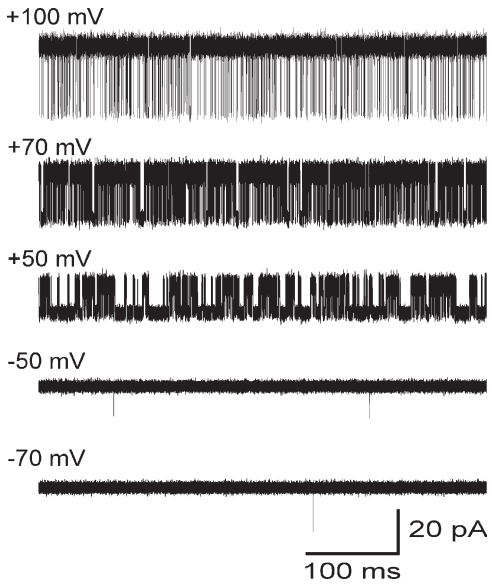

Figure 7. Simulated single-channel currents for Scheme V for BK_B channel DM4 at the indicated voltages with saturating Ca^{2+}_i. The simulated single-channel currents reproduce the kinetic properties of the experimental single-channel currents shown in Fig. 1.

TABLE III

Gating parameters determined from four BK_B channels as mean ± SEM

Parameter	Scheme IV	Scheme IV_F	Scheme V	Scheme V_F
A (s^{-1})	369 ± 163	384 ± 159	240 ± 136	397 ± 197
q_A (e_o)	0.470 ± 0.075	0.290 ± 0.075	0.355 ± 0.057	0.247 ± 0.063
B (s^{-1})	752 ± 215	1,090 ± 240	2,570 ± 1,190	1,700 ± 445
q_B (e_o)	−0.156 ± 0.090	−0.261 ± 0.074	−0.106 ± 0.053	−0.206 ± 0.077
H (s^{-1})	0.310 ± 0.196	0.824 ± 0.760	1.19 ± 0.569	1.23 ± 0.864
q_H (e_o)	0.197 ± 0.130	0.316 ± 0.064	0.116 ± 0.067	0.150 ± 0.090
K (s^{-1})	4,540 ± 1,250	5,030 ± 1,960	3,450 ± 1,160	2,030 ± 687
q_K (e_o)	−0.217 ± 0.091	−0.218 ± 0.052	−0.225 ± 0.103	−0.294 ± 0.142
D	22.9 ± 3.98	28.3 ± 2.15	17.9 ± 1.90	17.4 ± 2.20
E	0.997 ± 0.080	0.990 ± 0.097	1.37 ± 0.06	1.48 ± 0.061
U			4.13 ± 1.62	5.02 ± 3.24
W			1.31 ± 0.50	1.34 ± 0.39
H_F (s^{-1})		621 ± 88.6		603 ± 276
K_F (s^{-1})		21,200 ± 3,070		35,600 ± 19,600
q_G (e_o)	2.92 ± 0.59	2.74 ± 0.07	2.18 ± 0.15	2.26 ± 0.17

D, E, U, and W are without units. q_G = net gating charge = $4q_A - 4q_B + q_H - q_K$. The gating parameters are absent in the indicated kinetic schemes (blank cells).

idealized by being highly constrained (see schemes) with strict mathematical relationships determining the coupling and cooperative (when included) parameters. Because it is unlikely that a protein as complex as the BK_B channel would gate in the highly constrained manner defining these models, both the models and estimated parameters should be viewed as tools toward understand gating, rather than as actual gating mechanisms. The goal when examining the various models and parameters in the following sections is not to make fine distinctions among the models but to draw general conclusions that may apply to the underlying gating mechanism.

Estimates of partial charge movement

For the top-ranked Scheme V_F, the partial charge estimates for BK_B voltage sensor activation q_A of 0.247 ± 0.063 e_o and deactivation q_B of −0.206 ± 0.077 e_o (Table III) are consistent with those determined for wt BK channels by Horrigan and Aldrich (1999; 2002) of 0.33 and −0.22 e_o and Rothberg and Magleby (2000) of 0.285 and −0.215 e_o. (Note that the indicated values from Rothberg and Magleby [2000] were obtained by dividing q_1 and q_2 in their Table IV by 2.0 because in the simplified model they examined, there were only two voltage sensors instead of four.) The partial charge estimates in Table III for Scheme V_F for the closed to open transition, q_H = 0.150 ± 0.090 e_o, and for the open to closed transition, q_K = −0.294 ± 0.142 e_o, are consistent with the estimates determined by Horrigan and Aldrich (2002) of 0.22 and −0.145 e_o and Rothberg and Magleby (2000) of 0.03 ± 0.10 and −0.18 ± 0.05 e_o, respectively. The estimates of the partial charge movements for the other schemes are also generally consistent when the SEMs are taken into account. Thus, the estimates of partial charge associated with both voltage sensor movement and transitions between the open and closed states for BK_B channels are generally consistent with those for wt BK channels.

The effective charge movement for gating with each scheme was obtained by summing up the partial charges in the gating mechanisms for the movement of the voltage sensors ($4 \times q_A + 4 \times -q_B$) plus the partial charge movement associated with the opening and closing transitions ($q_H + -q_K$). For Scheme V_F, the total effective charge movement for the four examined channels was 2.26 ± 0.17 e_o (Table III), and the mean value for the four different gating schemes for the four channels was 2.52 ± 0.18 e_o. These values obtained from the voltage dependence of the various parameters in the kinetic schemes are consistent with the total effective charge movement from Table I of 2.29 ± 0.20 e_o determined from the slope of Po versus voltage. Fixing either one of the partial charge estimates for a single rate constant and then refitting indicated that changing one of the partial charges associated with a single rate constant (up to twofold with preservation of the sign) typically had small effects on the likelihoods as long as the total gating charge was preserved. This indicates that it is the total effective charge movement that is the most critical factor in the voltage dependence, as might be expected.

The total effective charge movements estimated for BK_B channels are also consistent with values reported for wt BK channels of 2.3 ± 0.6 e_o (Rothberg and Magleby, 2000) and 2.62 (Ma et al., 2006). Thus, to a first approximation, eliminating both the RCK1 Ca^{2+} sensor and the Mg^{2+} sensor through mutations to obtain BK_B channels does not change the effective gating charge of BK channels even though the data were obtained

in saturating Ca^{2+} for the Ca^{2+} bowl. This conclusion is consistent with previous findings that the voltage sensors and Ca^{2+} sensors of BK channels function relatively independently of one another (Cui and Aldrich, 2000; Rothberg and Magleby, 2000; Horrigan and Aldrich, 2002).

Coupling of the voltage sensors to channel opening and closing through *D* and *E*

For Schemes IV, IV_F, V, and V_F, each activated voltage sensor changes the C→O opening rate *D*-fold and the O→C closing rate *E*-fold. Values of *D* and *E* >1.0 would increase the transition rates, and values <1.0 would decrease them. For Schemes IV and IV_F, the voltage sensors are independent of one another, whereas for Schemes V and V_F, cooperative interactions through *U* and *W* are allowed among the voltage sensors. For Schemes IV, IV_F, V, and V_F, estimates of the coupling factor *D* were large, ranging from 17.4 to 28.3 (Table III), with a mean value for the four schemes of 21.6 ± 2.5. These estimates of *D* were significantly different from 1.0 ($P < 0.001$). A value of *D* of 21.6 would accelerate the opening rate 21.6-, 467-, 10,078-, and 217,678-fold for one, two, three, and four voltage sensors activated, respectively.

E for Schemes IV and IV_F was ∼0.99 ± 0.1 and not significantly different from 1.0, whereas *E* for Schemes V and V_F was ∼1.4 ± 0.1 and was significantly different from 1.0 ($P < 0.05$). An *E* of ∼0.99 would have a negligible effect on the channel closing rates, whereas an *E* of 1.4 would accelerate the closing rate 1.4-, 2.0-, 2.7-, and 3.8-fold for one, two, three, and four voltage sensors activated, respectively. Adding flicker closed states to Schemes IV and V to obtain Schemes IV_F and V_F had little effect on estimates of *D* or *E* (Table III).

At first it may seem paradoxical that voltage sensor activation may increase closing rates. However, the acceleration of the closing rate by *E* for Schemes V and V_F is small compared with the much larger effects of *D* on accelerating the opening rates (discussed above). Furthermore, the relative stability of the open and closed states depends on all of the rate constants in the kinetic scheme, with the rate constants being affected in a complex way by the various parameters (see Scheme V) and their voltage dependence. The net result is that voltage sensor activation does stabilize the open states, as measured by equilibrium occupancy. For example, for channel DM4 at 60 mV, the equilibrium occupancy of the open states with from zero to four voltage sensors activated is 0.000053, 0.00034, 0.0029, 0.037, and 0.63, respectively.

As discussed above and shown in Table III, our analysis determines separately the coupling of voltage sensor activation to both the opening C→O and closing O→C rates. The effect of voltage sensor activation on the C↔O equilibrium is given by $D_{HA} = D/E$, where D_{HA}, as defined by Horrigan and Aldrich (2002), indicates that the activation of each voltage sensor changes the C↔O equilibrium D_{HA}-fold. Calculating D_{HA} from the values of *D* and *E* in Table III gives estimates of D_{HA} of 23.0 and 28.6 for Schemes IV and IV_F, which have independent voltage sensors. When the SEMs of *D* and *E* in Table III are taken into account, these estimates are not different from the estimate for D_{HA} of 23.9 from Ma et al. (2006), which was also calculated assuming independent voltage sensors.

For Schemes V and V_F, which allow cooperativity among the voltage sensors, estimates of D_{HA} from the values of *D* and *E* in Table III were 13.1 for Scheme V and 11.7 for Scheme V_F. Thus, allowed voltage sensor cooperativity decreases the estimated magnitude of the coupling between voltage sensor activation and the C↔O equilibrium.

Independent of whether the schemes had independent voltage sensors (Schemes IV and IV_F) or cooperativity among voltage sensors (Schemes V and V_F), voltage sensor activation of the channel was mainly through coupling factor *D* accelerating the opening rates with minimal effect of coupling factor *E* on the closing rates.

Possible cooperativity among the voltage sensors through *U* and *W*

The estimates of cooperativity among the voltage sensors for Schemes V and V_F indicated that each activated voltage sensor accelerates the activation rate of the deactivated voltage sensors ∼4.6-fold and increases the deactivation rate of each activated voltage sensors ∼1.3-fold (mean of the values of *U* and *W* obtained from Schemes V and V_F in Table III). These estimates of *U* and *W* were not significantly different from 1.0 ($P > 0.1$) because of large SEMs. Nevertheless, allowing *U* and *W* cooperativity (compare Scheme V with Scheme IV and Scheme V_F with Scheme IV_F) led to significantly higher rankings for all four channels ($P < 0.001$; Table II and Table S4), which is consistent with possible cooperativity among voltage sensors for the examined models. In terms of Schemes V and V_F, one, two, and three activated voltage sensors would increase the activation of the deactivated voltage sensors 4.6-, 21.2-, and 97.3-fold, respectively, through *U* (based on the mean value of *U* for Schemes V and V_F), and one, two, and three deactivated voltage sensors would increase the deactivation rate of the activated sensors 1.3-, 1.7-, and 2.2-fold through *W* (based on the mean value of *W* for Schemes V and V_F). In terms of the models, cooperativity among voltage sensors greatly accelerates the activation of voltage sensors while having much less of an effect on their deactivation.

Constraining parameters indicates that estimates of *D*, *E*, *U*, and *W* are robust

The gating parameters in the kinetic schemes were typically free, with their values determined by the maximum

TABLE IV

Effect of constraining parameters on coupling and cooperativity[a]

Allosteric factors	No constraints on the gating parameters[b]	Constraints from Horrigan et al. (1999)[c]	Constraints from Fig. 2[d]
Scheme IV			
D	22.9 ± 4.0	21.9 ± 0.4	16.6 ± 1.8
E	0.997 ± 0.080	1.23 ± 0.47	1.00 ± 0.054
Scheme V			
D	17.4 ± 2.2	18.0 ± 2.6	12.9 ± 0.4
E	1.48 ± 0.06	1.41 ± 0.31	1.21 ± 0.13
U	5.02 ± 3.24	2.46 ± 0.57	4.27 ± 1.64
W	1.34 ± 0.39	1.27 ± 0.50	1.23 ± 0.38

[a]Values are the mean ± SEM for BK_B channels DM1–4.
[b]All the gating parameters in the indicated schemes were free, with their values determined by maximum likelihood fitting.
[c]q_a, q_b, q_H, and q_K were fixed to values in Horrigan et al. (1999) of 0.275 e_o, −0.275 e_o, 0.262 e_o, and −0.138 e_o, respectively.
[d]*H*, *K*, q_H, and q_K were fixed to the values from Fig. 2 of 3.85 s^{-1}, 6423 s^{-1}, 0.237 e_o, and −0.0994 e_o, respectively.

likelihood fitting process. We also examined whether fixing some of the parameters to values determined independently would lead to similar conclusions about coupling and cooperativity as those obtained with free parameters. Two examples are presented in Table IV for Schemes IV and V. Fixing q_a, q_b, q_H, and q_K to the values in Horrigan and Aldrich (1999) and then fitting gave coupling and cooperativity factors for Schemes IV and V that were not significantly different ($P > 0.4$) from those determined when the parameters were free (Table IV). Fixing *H*, *K*, q_H, and q_K to the values obtained in Fig. 2 also gave coupling and cooperativity factors that were not significantly different ($P > 0.09$ for each factor) from those determined when the parameters were not fixed (Table IV). No significance difference in the coupling and cooperativity factors for fixed versus free partial charges were also found (not depicted) when using fixed partial charges estimates from Rothberg and Magleby (2000) and from Horrigan and Aldrich (2002). Thus, fitting with some parameters fixed by independent estimates supports the conclusions from the free parameter fitting in the previous sections that coupling occurs mainly through *D* rather than *E* and that possible cooperativity occurs mainly through *U* and not *W*.

Comparison of models with cooperativity among voltage sensors to models with free parameters for each opening and closing rate

The results in the previous sections show that allowing cooperativity among the voltage sensors (Schemes V and V_F) can improve the description of the gating. Such an observation does not, of course, establish cooperativity but may simply reflect that additional free parameters can improve the description of the data or that the highly constrained idealized models force a distortion of some of the examined parameters from the true underlying parameters. Thus, the question arises whether relaxing constraints on factors other than cooperativity might also improve the description of the data.

To explore this possibility, we examined a new scheme in which the constraints on the strict coupling between voltage sensor activation and the opening/closing transitions were removed. To develop this new scheme, referred to as Scheme IV-free, *E*, E^2, E^3, E^4, *D*, D^2, D^3, and D^4 in Scheme IV were replaced with free rate constants E_0, E_1, E_2, E_3, D_0, D_1, D_2, and D_3, respectively, together with appropriate changes in the parameters for the O–O transitions to maintain microscopic reversibility. All opening rate constants in Scheme IV-free have the same partial charge movement incorporated through the voltage dependence of *K*, and all closing rate constants have the same partial charge movement incorporated through the voltage dependence of *H*. Scheme IV-free retains the independent voltage sensor activation found in Scheme IV. Scheme IV-free was then compared with Scheme V, which has cooperativity among the voltage sensors. Scheme IV-free ranked below Scheme V for all channels (Table S5, top pairing). Therefore, for these two 10-state schemes, a model with cooperativity among voltage sensors is preferred over a model with free rate constants for the opening and closing transitions.

For 15-state models, Scheme IV_F-free (Scheme IV-free with added flickers) ranked below Scheme V_F for two channels and above Scheme V_F for the other two channels (Table S5, middle pairing). Thus, for models with flickers, the rankings give no preference between models with unconstrained coupling or with cooperativity among voltage sensors. For both Scheme IV-free and Scheme IV_F-free, the opening rates still increased with a power approximated by the number of activated voltage sensors, with the free coupling typically making minor adjustments in the opening rates compared with the constrained models. Thus, the basic features of the gating were preserved.

Interestingly, starting with Scheme IV_F-free and also allowing cooperativity among voltage sensors to obtain Scheme V_F-free allowed Scheme V_F-free to rank above Scheme IV_F-free for all four channels (Table S5, bottom

pairing), consistent with, but not establishing, cooperativity among voltage sensors for the examined models.

The gating with free coupling between voltage sensors and the opening/closing transitions was consistent with the major conclusions from the previous sections: voltage sensor activation still increased Po mainly through increases in the opening rates, with limited effects on the closing rate constants; and models with allowed cooperativity among voltage sensors ranked above the same models without such cooperativity. A difficulty with relaxed constraints on the coupling is that the resulting extra free parameters can lead to several of the free parameters being poorly defined, rendering the models of limited use for structure/function studies. Schemes V and V_F with fewer free parameters already provide an adequate description of the data and should be suitable for such studies.

DISCUSSION

In this study, we examine possible allosteric coupling and cooperative factors involved in the voltage-dependent gating of a simplified BK channel, BK_B, with only one Ca^{2+} binding site (the Ca^{2+} bowl) per subunit. The Ca^{2+} bowl was then saturated with Ca^{2+} to drive the gating into the 10-state two-tiered model in Scheme II. The simplified BK_B channels with saturating Ca^{2+} were used to increase the activity sufficiently so that single-channel data could be collected over a wide range of Po and voltage. Single-channel data provided a means to test the ability of the various models to account for the detailed gating kinetics and also to facilitate the estimation of rate constants rather than equilibrium constants. The results of our study indicate that the steady-state voltage-dependent single-channel kinetics of BK_B channels is not described by Scheme III, can be approximated by Schemes IV and IV_F, and are well described by Schemes V and V_F.

Scheme III, a highly constrained MWC-like model (Monod et al., 1965; Fersht, 1985) with voltage sensors rather than ligand sensors and with no allosteric coupling between voltage sensors and the opening and closing transitions rates, could, rather surprisingly, provide a description of the voltage dependence of the open distributions and could also approximate Po over limited ranges of voltage. However, Scheme III did not even come close to approximating the voltage dependence of the closed time distributions (Figs. 4 and 5, dashed blue lines). Clearly, an MWC-like model without coupling of the voltage sensors to the opening and closing transitions is inconsistent with the single-channel kinetics. (These findings with Scheme III also illustrate that the ability to approximate Po on a linear plot does not necessarily provide a critical test of a model. Such tests must explore wide ranges of voltage, including very low Po's.)

Allowing allosteric coupling between voltage sensors and channel opening and closing (Schemes IV and IV_F) based on highly constrained and idealized allosteric models considered previously (Marks and Jones, 1992; Ríos et al., 1993; McCormack et al., 1994; Horrigan et al., 1999; Horrigan and Aldrich, 2002) gave greatly improved descriptions of the gating. In these models, we used separate allosteric factors for coupling voltage sensor movement to the opening (D) and closing (E) transitions rather than an equilibrium coupling factor. The highly constrained Scheme IV captured the major features of the voltage dependence of Po and the single channel data, but with some noticeable errors in Po at very negative potentials and in the closed dwell-time distribution (Figs. 4 and 5). The constraints in Scheme IV reduced the number of gating parameters to 10 (the coupling factors D and E and the rate constants A, B, K, and H and their associated voltage dependence). Without any constraints there would be 48 free parameters: 26 rate constants with two parameters each to define the rate constants at 0 mV and their voltage dependence, minus one parameter in each of the four loops to constrain microscopic reversibility. The rather amazing finding is that the highly constrained Scheme IV with only 10 free parameters compared with approximately five times that number if all were free could approximate the voltage dependence of Po and capture the major features of the single-channel kinetics, as revealed through the open and closed dwell-time distributions.

For Scheme IV, the allosteric factor D increased the opening rate an additional 22.9-fold for each activated voltage sensor (Table III). One to four activated voltage sensors would then accelerate the opening rate 22.9-, 524-, 12,000-, and 275,000-fold, respectively. The allosteric coupling factor E for channel closing was ~1.0, so there would be little effect of voltage sensors on the closing rates. Thus, changes in the open–close equilibrium coupling factor D_{HA} of Horrigan and Aldrich (2002) would arise through changes in the opening rate. Consequently, our allosteric coupling factor D for opening of 22.9 ± 4.0 for Scheme IV can be compared directly with, and is not significantly different from, estimates of the equilibrium allosteric coupling factor D_{HA}, which ranged from 23.9 to 25 (Horrigan and Aldrich, 2002; Ma et al., 2006; Horrigan and Ma, 2008). Estimates of D_{HA} for Scheme IV and those by Horrigan and co-workers were determined assuming no cooperative interactions among voltage sensors.

Allowing cooperativity in activation of voltage sensors with Scheme V further improved the description of the data so that the predictions with Scheme V essentially superimposed both the voltage dependence of the experimentally observed Po and also the dwell-time histograms (Figs. 4 and 5). For Scheme V, each activated voltage sensor increased the activation rate of

the remaining voltage sensors 4.1 ± 1.6-fold (U) with little effect (1.3 ± 0.5) on the deactivation rate (W). With this allowed cooperativity among the voltage sensors, estimates of D were decreased from 23 to 17.5, and estimates of E were increased from 1.0 to 1.4, changing D_{HA} from 23 to 12.5. Thus, if cooperativity among voltage sensors is present but not included in models, the models can compensate by changing the coupling factors to increase the D_{HA}. Thus, voltage sensor cooperativity, if present, could masquerade as an increased coupling factor if voltage sensor cooperativity is not included in the model.

Consistent with the possibility of cooperativity in activation of voltage sensors in BK channels, Horrigan and Aldrich (2002) cleverly deduced a possible calcium-dependent cooperativity in voltage-sensor movement for wt BK channels from limiting slope analysis of Po (their Fig. 12). If the structure and position of each voltage sensor domain (S1–S4) in BK channels is similar to that in Kv1.2 channels, the S4 segments of the voltage sensors would be separated from one another and unlikely to interact directly (Long et al., 2005a,b; Horn, 2009). Nevertheless, the S4–S5 linker of each voltage sensor in Kv1.2 runs underneath a neighboring subunit to connect to S5, allowing intersubunit interactions (Tombola et al., 2006). In addition, retrograde action on the voltage sensors is possible through possible cooperative changes in tension on the S4–S5 linkers. For BK channels, the large intracellular gating ring may also interact with intracellular parts of the voltage sensor and the S4–S5 linker, providing more points for interactions (Horrigan and Ma, 2008; Yang et al., 2008).

The possible voltage sensor cooperativity observed by Horrigan and Aldrich (2002) was Ca^{2+} dependent, requiring saturating Ca^{2+} for the two high affinity Ca^{2+} sites per subunit on the wt channels in their experiments. In addition, the cooperativity we observed was in saturating Ca^{2+} for the one high affinity Ca^{2+} site per subunit for the BK_B channels in our experiments, implicating an activated gating ring in the cooperativity among voltage sensors. Previous studies suggest that Ca^{2+} expands the gating ring, increasing Po by perhaps pulling on the S6 gates through gating ring–S6 linkers (Jiang et al., 2002; Niu et al., 2004; Dong et al., 2005; Ye et al., 2006; Lingle, 2007). Therefore, Ca^{2+}-dependent cooperativity in voltage sensor activation for BK channels may be associated with or require an expanded gating ring that interacts with the voltage sensors/S4–S5 linkers, allowing cooperativity in some manner, or instead, the expanded gating ring may apply increased opening tension on the RCK1-S6 linkers, which could facilitate the cooperative movement of the voltage sensors in some manner.

As mentioned previously, our observation that allowing voltage sensor cooperativity leads to higher ranking models is consistent with, but does not establish, voltage sensor cooperativity. In principle, direct measurement of gating currents could reveal voltage sensor cooperativity. Scheme IV (without cooperativity among voltage sensors) with the parameters in Table III predicts that gating currents should be at maximum immediately after the voltage step and then decay thereafter, whereas Scheme V with cooperativity among voltage sensors and the parameters in Table III predicts a delay to peak gating currents of ~35 µs followed by a decay (determined by tabulating partial charge movement during simulation of single-channel gating). The gating currents for wt BK channels in Horrigan and Aldrich (1999) show a delay to peak, but this delay arises from the filtering associated with the experimentation, as Horrigan and Aldrich (1999) show in their Fig. 9.

Alternatively, it is possible that the mutated BK channel and 95 µM Ca^{2+} used in our analysis induces cooperativity among voltage sensors that would be absent in the Horrigan and Aldrich (1999) measurements of gating currents in wt BK channels performed in 0 Ca^{2+}. Consistent with this possibility, the study of Horrigan and Aldrich (2002) suggests possible cooperativity in voltage sensor activation for wt BK channels gating in Ca^{2+}. This cooperativity was based on estimates of open-channel charge movement, raising the possibility that voltage sensor activation may be cooperative only when channels are open. If this is the case, the absence of a delay in the ON gating current would not exclude cooperativity interactions. Gating current experiments on BK_B channels in 95 µM Ca^{2+} should allow resolution of the question of possible cooperativity among voltage sensor activation under the conditions of our experiments. Depending on the findings, the idealized models could be modified to be consistent with the observed gating currents and then retested.

BK channels differ from Shaker Kv channels in that BK channels can open with zero to four voltage sensors activated (Stefani et al., 1997; Horrigan and Aldrich, 1999, 2002), as depicted in Schemes I–V. In contrast, Shaker Kv channels typically open after all four voltage sensors are activated (Zagotta et al., 1994; Schoppa and Sigworth, 1998; Gagnon and Bezanilla, 2009). Possible cooperativity among voltage sensors in Shaker channels, if present, is probably not pronounced, with reports of a small negative (Zagotta et al., 1994), a small positive (Schoppa and Sigworth, 1998), or negligible (Gagnon and Bezanilla, 2009; Horn, 2009) cooperativity, depending on the specific models and experiments. Cui et al. (2009) argue that similar basic mechanisms in voltage-dependent gating may apply to both BK and Kv channels but that unique structural features in BK channels may give rise to some differences.

Previous studies on BK channels have suggested the presence of flicker (brief duration) closed states (Rothberg and Magleby, 1998, 1999). Consistent with this finding,

the addition of flicker closed states to the constrained models to obtain Schemes IV_F and V_F significantly improved the description of the data. Such flicker closed states may arise from instability in the selectivity filter (Piskorowski and Aldrich, 2006; Schroeder and Hansen, 2007, 2008). It should be noted that the physical basis of the actual gate in BK channels is not clear (Piskorowski and Aldrich, 2006; Wilkens and Aldrich, 2006; Cui et al., 2009; Wu et al., 2009). Although the flicker states in Schemes IV_F and V_F were add-on states with flicker closing after opening, flicker states interposed between the closed and open states are also consistent with gating of BK channels (Rothberg and Magleby, 1999). Consequently, we cannot exclude that the flicker closed states are interposed between the closed and open states. Acetylcholine receptor channels also have flicker closed states (referred to as flipped or primed states) interposed between the closed and open states (Lape et al., 2008; Mukhtasimova et al., 2009).

In our analysis, the assumption was made that saturating the Ca^{2+} bowl on the BK_B channel with high Ca^{2+} would drive the gating into the right-most 10 states, as in Scheme II. In practice, no matter how high the free Ca^{2+}, Ca^{2+} would still dissociate from the binding sites and then, assuming an on rate of 3×10^8 M^{-1} s^{-1} (Fersht, 1985), rebind after, on average, ~30 µs for 100 µM Ca^{2+}. These brief unbindings should have minimal effects on the gating. To test this assumption, the data that were simultaneously fit for channel DM4 were also simultaneously fit with the 50-state Scheme I with the constraints of Scheme IV for the voltage-dependent gating. The Ca^{2+} on rate was fixed at 3×10^8 M^{-1} s^{-1}, and the Ca^{2+}_i was fixed at 95 µM. The Ca^{2+} off rate determined by fitting was ~418/s. Typically, ~95% of the state occupancy was in the right-most 10 states in Scheme 1, with only ~5% in the 10 states immediately to the left of the right-most states and <0.1% in the states further to the left. Estimates of the coupling and cooperative factors were little affected by allowing Ca^{2+} to unbind and rebind. Consequently, as a first approximation, the assumption that the gating is confined to the right-most 10 states appears suitable for the questions being addressed in our study.

If it is assumed that the actual underlying gating mechanism of BK_B channels in saturating Ca^{2+} is generally consistent with Schemes IV, IV_F, V, and V_F, what does this tell us about mechanism? Consider Scheme IV, in which the coupling factor for *D* was ~23 and the coupling factor for *E* was ~1 (Table III). In terms of the examined highly constrained idealized models, these values indicate that the opening rate increases *D*-fold with each additional activated voltage sensor, whereas the closing rate remains relatively constant, independent of voltage sensor position. This suggests, in terms of the models, that the energy barrier for channel opening decreases with each additional activated voltage sensor, whereas the energy barrier for channel closing is little altered by voltage sensor movement. Where are these energy barriers? BK channels, like most channels, are bistable (typically open or closed), such that the time spent in transitioning between open and closed states is insignificant compared with the total time spent in the open and closed states. Bistable gating would be consistent with latch (or spring loaded) mechanisms forming the energy barriers to stabilize the closed and open states (Niu et al., 2004; Kahlig et al., 2006; Purohit and Auerbach, 2007; Wu et al., 2009).

BK channels can gate in the absence of Ca^{2+} and at very negative potentials where the voltage sensors are held in the deactivated position (Horrigan and Aldrich, 2002). Thus, thermal energy is sufficient to disrupt the closed latch and move the gate over to the open latch, even when no voltage or Ca^{2+} sensors are activated. In terms of Schemes IV and V, activated voltage sensors could then speed up the opening by reducing the strength of the closed latches or by applying a force to help pull the gates off the closed latches so that less thermal energy would be needed to disrupt the closed latches. In contrast (in terms of these specific schemes), activated voltage sensors would have little effect on the strength of the open latches or the forces acting to close open gates.

The properties of gating imposed by Schemes IV and V on BK channels have some features in common with a standard toggle switch. Both are bistable processes. For the toggle switch, a bistable spring mechanism holds the contacts either open or closed. For the BK channel, a bistable mechanism (springs and/or latches?) holds the gates either open or closed. For both of these switching devices, the time spent in transition between the two bistable states is insignificant compared with the time spent in the states. For the toggle switch, the absolute magnitudes of the (finger) forces required to either open or close the switch are typically identical. For the BK channel, the effective amount of energy required to open a channel at low Po's can be orders of magnitude greater than the amount of energy required to close the same channel. Depolarization (and Ca^{2+}_i) then decreases the force required to open the channel while having much less of an effect on the force required to close the channel; at intermediate Po's, the opening and closing forces can be about the same (like a toggle switch), whereas at very high Po's, the opening force can be less than the closing force. Thus, BK channels can be viewed as a toggle switch with differential switching forces, depending on the conditions.

It is unlikely that a protein as complex as the BK or BK_B channel would gate with the exact constraints imposed by the examined idealized gating mechanisms, and previous studies suggest some deviations from the constraints imposed by these schemes (Horrigan et al., 1999; Rothberg and Magleby, 2000; Horrigan and

Aldrich, 2002; Qian et al., 2006). Consequently, the gating schemes tested in this study are, at best, approximations to the underlying gating mechanism. Nevertheless, the examined gating mechanisms are consistent with the quaternary structure of BK channels, the top-rated gating mechanisms approximate the voltage dependence of the steady-state single-channel gating kinetics over a 10,000-fold range in Po, and there is reasonable agreement between many of the gating parameters estimated in this study when compared with estimates from previous studies obtained with different experimental approaches (Rothberg and Magleby, 2000; Horrigan and Aldrich, 2002; Ma et al., 2006; Horrigan and Ma, 2008).

One advantage of the constrained models is that the number of free parameters is greatly reduced compared with models without constraints. This facilitates both estimation of the parameters and also comparison of parameters obtained under different experimental conditions or for structurally modified channels. A further advantage of constrained models is that they augment thinking in terms of underlying gating mechanism. A constrained model defines the gating for an idealized mechanism. To the extent that the gating deviates from the idealized mechanism, then this suggests additional aspects of gating that need to be included. These additional aspects can then be included and the whole process repeated iteratively until the developed gating mechanism can account for all aspects of the data. Gating would then be defined in terms of idealized models and deviations from those models.

This study was supported in part by an American Heart Association fellowship and a Lois Pope fellowship to C. Shelley, an American Heart Association fellowship to Y. Geng, and National Institutes of Health grant AR032805 to K.L. Magleby. The contents of this manuscript are solely the responsibility of the authors and do not necessarily represent the official views of the agencies providing fellowship and grant support.

Christopher Miller served as editor.

Submitted: 23 September 2009
Accepted: 10 March 2010

REFERENCES

Adelman, J.P., K.Z. Shen, M.P. Kavanaugh, R.A. Warren, Y.N. Wu, A. Lagrutta, C.T. Bond, and R.A. North. 1992. Calcium-activated potassium channels expressed from cloned complementary DNAs. *Neuron.* 9:209–216. doi:10.1016/0896-6273(92)90160-F

Bao, L., A.M. Rapin, E.C. Holmstrand, and D.H. Cox. 2002. Elimination of the BK_{Ca} channel's high-affinity Ca^{2+} sensitivity. *J. Gen. Physiol.* 120:173–189. doi:10.1085/jgp.20028627

Bao, L., C. Kaldany, E.C. Holmstrand, and D.H. Cox. 2004. Mapping the BKCa channel's "Ca^{2+} bowl": side-chains essential for Ca^{2+} sensing. *J. Gen. Physiol.* 123:475–489. doi:10.1085/jgp.200409052

Barrett, J.N., K.L. Magleby, and B.S. Pallotta. 1982. Properties of single calcium-activated potassium channels in cultured rat muscle. *J. Physiol.* 331:211–230.

Bello, R.A., and K.L. Magleby. 1998. Time-irreversible subconductance gating associated with Ba^{2+} block of large conductance Ca^{2+}-activated K^+ channels. *J. Gen. Physiol.* 111:343–362. doi:10.1085/jgp.111.2.343

Butler, A., S. Tsunoda, D.P. McCobb, A. Wei, and L. Salkoff. 1993. mSlo, a complex mouse gene encoding "maxi" calcium-activated potassium channels. *Science.* 261:221–224. doi:10.1126/science.7687074

Colquhoun, D., and A.G. Hawkes. 1995. The principles of the stochastic interpretation of ion-channel mechanisms. *In* Single Channel Recording. B. Sakmann and E. Neher, editors. Plenum Press, New York. 397–482.

Cox, D.H., J. Cui, and R.W. Aldrich. 1997. Allosteric gating of a large conductance Ca-activated K^+ channel. *J. Gen. Physiol.* 110:257–281. doi:10.1085/jgp.110.3.257

Crouzy, S.C., and F.J. Sigworth. 1990. Yet another approach to the dwell-time omission problem of single-channel analysis. *Biophys. J.* 58:731–743. doi:10.1016/S0006-3495(90)82416-4

Cui, J., and R.W. Aldrich. 2000. Allosteric linkage between voltage and Ca^{2+}-dependent activation of BK-type mslo1 K^+ channels. *Biochemistry.* 39:15612–15619. doi:10.1021/bi001509+

Cui, J., D.H. Cox, and R.W. Aldrich. 1997. Intrinsic voltage dependence and Ca^{2+} regulation of mslo large conductance Ca-activated K^+ channels. *J. Gen. Physiol.* 109:647–673. doi:10.1085/jgp.109.5.647

Cui, J., H. Yang, and U.S. Lee. 2009. Molecular mechanisms of BK channel activation. *Cell. Mol. Life Sci.* 66:852–875. doi:10.1007/s00018-008-8609-x

Diaz, F., M. Wallner, E. Stefani, L. Toro, and R. Latorre. 1996. Interaction of internal Ba^{2+} with a cloned Ca^{2+}-dependent K^+ (hslo) channel from smooth muscle. *J. Gen. Physiol.* 107:399–407. doi:10.1085/jgp.107.3.399

Díaz, L., P. Meera, J. Amigo, E. Stefani, O. Alvarez, L. Toro, and R. Latorre. 1998. Role of the S4 segment in a voltage-dependent calcium-sensitive potassium (hSlo) channel. *J. Biol. Chem.* 273:32430–32436. doi:10.1074/jbc.273.49.32430

Dong, J., N. Shi, I. Berke, L. Chen, and Y. Jiang. 2005. Structures of the MthK RCK domain and the effect of Ca^{2+} on gating ring stability. *J. Biol. Chem.* 280:41716–41724. doi:10.1074/jbc.M508144200

Fersht, A. 1985. Enzyme Structure and Mechanism. Second edition. W.H. Freeman and Company, New York. 149 pp.

Fredkin, D.R., M. Montal, and J.A. Rice. 1985. Identification of aggregated Markovian models: application to the nicotinic acetylcholine receptor. *In* Proceedings of the Berkeley Conference in Honor of Jerzy Neyman and Jack Kiefer. L.M. LeCam and R.A. Olshen, editors. Wadsworth Advanced Books & Software, Monterey, CA. 269–289.

Gagnon, D.G., and F. Bezanilla. 2009. A single charged voltage sensor is capable of gating the Shaker K^+ channel. *J. Gen. Physiol.* 133:467–483. doi:10.1085/jgp.200810082

Gil, Z., K.L. Magleby, and S.D. Silberberg. 2001. Two-dimensional kinetic analysis suggests nonsequential gating of mechanosensitive channels in *Xenopus* oocytes. *Biophys. J.* 81:2082–2099. doi:10.1016/S0006-3495(01)75857-2

Horn, R. 2009. Uncooperative voltage sensors. *J. Gen. Physiol.* 133:463–466. doi:10.1085/jgp.200910236

Horn, R., and K. Lange. 1983. Estimating kinetic constants from single channel data. *Biophys. J.* 43:207–223. doi:10.1016/S0006-3495(83)84341-0

Horrigan, F.T., and R.W. Aldrich. 1999. Allosteric voltage gating of potassium channels II. Mslo channel gating charge movement in the absence of Ca^{2+}. *J. Gen. Physiol.* 114:305–336. doi:10.1085/jgp.114.2.305

Horrigan, F.T., and R.W. Aldrich. 2002. Coupling between voltage sensor activation, Ca^{2+} binding and channel opening in large

conductance (BK) potassium channels. *J. Gen. Physiol.* 120:267–305. doi:10.1085/jgp.20028605

Horrigan, F.T., and Z. Ma. 2008. Mg^{2+} enhances voltage sensor/gate coupling in BK channels. *J. Gen. Physiol.* 131:13–32. doi:10.1085/jgp.200709877

Horrigan, F.T., J. Cui, and R.W. Aldrich. 1999. Allosteric voltage gating of potassium channels I. Mslo ionic currents in the absence of Ca^{2+}. *J. Gen. Physiol.* 114:277–304. doi:10.1085/jgp.114.2.277

Jiang, Y., A. Pico, M. Cadene, B.T. Chait, and R. MacKinnon. 2001. Structure of the RCK domain from the E. coli K^+ channel and demonstration of its presence in the human BK channel. *Neuron.* 29:593–601. doi:10.1016/S0896-6273(01)00236-7

Jiang, Y., A. Lee, J. Chen, M. Cadene, B.T. Chait, and R. MacKinnon. 2002. Crystal structure and mechanism of a calcium-gated potassium channel. *Nature.* 417:515–522. doi:10.1038/417515a

Kahlig, K.M., S.N. Misra, and A.L. George Jr. 2006. Impaired inactivation gate stabilization predicts increased persistent current for an epilepsy-associated SCN1A mutation. *J. Neurosci.* 26:10958–10966. doi:10.1523/JNEUROSCI.3378-06.2006

Koehler, A.B., and E.H. Murphree. 1988. A comparison of the Akaike and Schwarz Criteria for selecting model order. *Appl. Stat.* 37:187–195. doi:10.2307/2347338

Lape, R., D. Colquhoun, and L.G. Sivilotti. 2008. On the nature of partial agonism in the nicotinic receptor superfamily. *Nature.* 454:722–727.

Latorre, R., and S. Brauchi. 2006. Large conductance Ca^{2+}-activated K^+ (BK) channel: activation by Ca^{2+} and voltage. *Biol. Res.* 39:385–401. doi:10.4067/S0716-97602006000300003

Lingle, C.J. 2007. Gating rings formed by RCK domains: keys to gate opening. *J. Gen. Physiol.* 129:101–107. doi:10.1085/jgp.200709739

Long, S.B., E.B. Campbell, and R. Mackinnon. 2005a. Crystal structure of a mammalian voltage-dependent Shaker family K^+ channel. *Science.* 309:897–903. doi:10.1126/science.1116269

Long, S.B., E.B. Campbell, and R. Mackinnon. 2005b. Voltage sensor of Kv1.2: structural basis of electromechanical coupling. *Science.* 309:903–908. doi:10.1126/science.1116270

Lu, R., A. Alioua, Y. Kumar, M. Eghbali, E. Stefani, and L. Toro. 2006. MaxiK channel partners: physiological impact. *J. Physiol.* 570:65–72. doi:10.1113/jphysiol.2005.098913

Ma, Z., X.J. Lou, and F.T. Horrigan. 2006. Role of charged residues in the S1-S4 voltage sensor of BK channels. *J. Gen. Physiol.* 127:309–328. doi:10.1085/jgp.200509421

Magleby, K.L. 2003. Gating mechanism of BK (Slo1) channels: so near, yet so far. *J. Gen. Physiol.* 121:81–96. doi:10.1085/jgp.20028721

Magleby, K.L., and L. Song. 1992. Dependency plots suggest the kinetic structure of ion channels. *Proc. R. Soc. Lond. B Biol. Sci.* 249:133–142. doi:10.1098/rspb.1992.0095

Marks, T.N., and S.W. Jones. 1992. Calcium currents in the A7r5 smooth muscle-derived cell line. An allosteric model for calcium channel activation and dihydropyridine agonist action. *J. Gen. Physiol.* 99:367–390. doi:10.1085/jgp.99.3.367

McCormack, K., W.J. Joiner, and S.H. Heinemann. 1994. A characterization of the activating structural rearrangements in voltage-dependent Shaker K^+ channels. *Neuron.* 12:301–315. doi:10.1016/0896-6273(94)90273-9

McManus, O.B., and K.L. Magleby. 1988. Kinetic states and modes of single large-conductance calcium-activated potassium channels in cultured rat skeletal muscle. *J. Physiol.* 402:79–120.

McManus, O.B., and K.L. Magleby. 1989. Kinetic time constants independent of previous single-channel activity suggest Markov gating for a large conductance Ca-activated K channel. *J. Gen. Physiol.* 94:1037–1070. doi:10.1085/jgp.94.6.1037

McManus, O.B., and K.L. Magleby. 1991. Accounting for the Ca^{2+}-dependent kinetics of single large-conductance Ca^{2+}-activated K^+ channels in rat skeletal muscle. *J. Physiol.* 443:739–777.

Meera, P., M. Wallner, M. Song, and L. Toro. 1997. Large conductance voltage- and calcium-dependent K^+ channel, a distinct member of voltage-dependent ion channels with seven N-terminal transmembrane segments (S0-S6), an extracellular N terminus, and an intracellular (S9-S10) C terminus. *Proc. Natl. Acad. Sci. USA.* 94:14066–14071. doi:10.1073/pnas.94.25.14066

Monod, J., J. Wyman, and J.P. Changeux. 1965. On the nature of allosteric transitions: a plausible model. *J. Mol. Biol.* 12:88–118. doi:10.1016/S0022-2836(65)80285-6

Mukhtasimova, N., W.Y. Lee, H.L. Wang, and S.M. Sine. 2009. Detection and trapping of intermediate states priming nicotinic receptor channel opening. *Nature.* 459:451–454. doi:10.1038/nature07923

Nimigean, C.M., and K.L. Magleby. 1999. The β subunit increases the Ca^{2+} sensitivity of large conductance Ca^{2+}-activated potassium channels by retaining the gating in the bursting states. *J. Gen. Physiol.* 113:425–440. doi:10.1085/jgp.113.3.425

Niu, X., and K.L. Magleby. 2002. Stepwise contribution of each subunit to the cooperative activation of BK channels by Ca^{2+}. *Proc. Natl. Acad. Sci. USA.* 99:11441–11446. doi:10.1073/pnas.172254699

Niu, X., X. Qian, and K.L. Magleby. 2004. Linker-gating ring complex as passive spring and Ca^{2+}-dependent machine for a voltage and Ca^{2+}-activated potassium channel. *Neuron.* 42:745–756.

Piskorowski, R.A., and R.W. Aldrich. 2006. Relationship between pore occupancy and gating in BK potassium channels. *J. Gen. Physiol.* 127:557–576. doi:10.1085/jgp.200509482

Purohit, P., and A. Auerbach. 2007. Acetylcholine receptor gating at extracellular transmembrane domain interface: the "pre-M1" linker. *J. Gen. Physiol.* 130:559–568. doi:10.1085/jgp.200709857

Qian, X., X. Niu, and K.L. Magleby. 2006. Intra- and intersubunit cooperativity in activation of BK channels by Ca^{2+}. *J. Gen. Physiol.* 128:389–404. doi:10.1085/jgp.200609486

Ríos, E., M. Karhanek, J. Ma, and A. González. 1993. An allosteric model of the molecular interactions of excitation-contraction coupling in skeletal muscle. *J. Gen. Physiol.* 102:449–481. doi:10.1085/jgp.102.3.449

Rothberg, B.S., and K.L. Magleby. 1998. Kinetic structure of large-conductance Ca^{2+}-activated K^+ channels suggests that the gating includes transitions through intermediate or secondary states. A mechanism for flickers. *J. Gen. Physiol.* 111:751–780. doi:10.1085/jgp.111.6.751

Rothberg, B.S., and K.L. Magleby. 1999. Gating kinetics of single large-conductance Ca^{2+}-activated K^+ channels in high Ca^{2+} suggest a two-tiered allosteric gating mechanism. *J. Gen. Physiol.* 114:93–124. doi:10.1085/jgp.114.1.93

Rothberg, B.S., and K.L. Magleby. 2000. Voltage and Ca^{2+} activation of single large-conductance Ca^{2+}-activated K^+ channels described by a two-tiered allosteric gating mechanism. *J. Gen. Physiol.* 116:75–99. doi:10.1085/jgp.116.1.75

Rothberg, B.S., R.A. Bello, and K.L. Magleby. 1997. Two-dimensional components and hidden dependencies provide insight into ion channel gating mechanisms. *Biophys. J.* 72:2524–2544. doi:10.1016/S0006-3495(97)78897-0

Salkoff, L., A. Butler, G. Ferreira, C. Santi, and A. Wei. 2006. High-conductance potassium channels of the SLO family. *Nat. Rev. Neurosci.* 7:921–931. doi:10.1038/nrn1992

Savalli, N., A. Kondratiev, L. Toro, and R. Olcese. 2006. Voltage-dependent conformational changes in human $Ca^{(2+)}$- and voltage-activated $K^{(+)}$ channel, revealed by voltage-clamp fluorometry. *Proc. Natl. Acad. Sci. USA.* 103:12619–12624. doi:10.1073/pnas.0601176103

Schoppa, N.E., and F.J. Sigworth. 1998. Activation of Shaker potassium channels. III. An activation gating model for wild-type and V2 mutant channels. *J. Gen. Physiol.* 111:313–342. doi:10.1085/jgp.111.2.313

Schreiber, M., and L. Salkoff. 1997. A novel calcium-sensing domain in the BK channel. *Biophys. J.* 73:1355–1363. doi:10.1016/S0006-3495(97)78168-2

Schroeder, I., and U.P. Hansen. 2007. Saturation and microsecond gating of current indicate depletion-induced instability of the MaxiK selectivity filter. *J. Gen. Physiol.* 130:83–97. doi:10.1085/jgp.200709802

Schroeder, I., and U.P. Hansen. 2008. Tl^+-induced micros gating of current indicates instability of the MaxiK selectivity filter as caused by ion/pore interaction. *J. Gen. Physiol.* 131:365–378. doi:10.1085/jgp.200809956

Shi, J., G. Krishnamoorthy, Y. Yang, L. Hu, N. Chaturvedi, D. Harilal, J. Qin, and J. Cui. 2002. Mechanism of magnesium activation of calcium-activated potassium channels. *Nature.* 418:876–880. doi:10.1038/nature00941

Song, L., and K.L. Magleby. 1994. Testing for microscopic reversibility in the gating of maxi K^+ channels using two-dimensional dwell-time distributions. *Biophys. J.* 67:91–104. doi:10.1016/S0006-3495(94)80458-8

Stefani, E., M. Ottolia, F. Noceti, R. Olcese, M. Wallner, R. Latorre, and L. Toro. 1997. Voltage-controlled gating in a large conductance Ca^{2+}-sensitive K^+ channel (hslo). *Proc. Natl. Acad. Sci. USA.* 94:5427–5431. doi:10.1073/pnas.94.10.5427

Tombola, F., M.M. Pathak, and E.Y. Isacoff. 2006. How does voltage open an ion channel? *Annu. Rev. Cell Dev. Biol.* 22:23–52. doi:10.1146/annurev.cellbio.21.020404.145837

Wilkens, C.M., and R.W. Aldrich. 2006. State-independent block of BK channels by an intracellular quaternary ammonium. *J. Gen. Physiol.* 128:347–364. doi:10.1085/jgp.200609579

Wu, Y., Y. Xiong, S. Wang, H. Yi, H. Li, N. Pan, F.T. Horrigan, Y. Wu, and J. Ding. 2009. Intersubunit coupling in the pore of BK channels. *J. Biol. Chem.* 284:23353–23363.

Xia, X.M., X. Zeng, and C.J. Lingle. 2002. Multiple regulatory sites in large-conductance calcium-activated potassium channels. *Nature.* 418:880–884. doi:10.1038/nature00956

Yang, H., J. Shi, G. Zhang, J. Yang, K. Delaloye, and J. Cui. 2008. Activation of Slo1 BK channels by Mg^{2+} coordinated between the voltage sensor and RCK1 domains. *Nat. Struct. Mol. Biol.* 15:1152–1159. doi:10.1038/nsmb.1507

Ye, S., Y. Li, L. Chen, and Y. Jiang. 2006. Crystal structures of a ligand-free MthK gating ring: insights into the ligand gating mechanism of K^+ channels. *Cell.* 126:1161–1173. doi:10.1016/j.cell.2006.08.029

Zagotta, W.N., T. Hoshi, and R.W. Aldrich. 1994. Shaker potassium channel gating. III: Evaluation of kinetic models for activation. *J. Gen. Physiol.* 103:321–362. doi:10.1085/jgp.103.2.321

Zeng, X.H., X.M. Xia, and C.J. Lingle. 2005. Divalent cation sensitivity of BK channel activation supports the existence of three distinct binding sites. *J. Gen. Physiol.* 125:273–286. doi:10.1085/jgp.200409239